



Nordic Council
of Ministers

Revising PM_{2.5} emissions from residential combustion, 2005– 2019

Implications for air quality concentrations and trends



Revising PM_{2.5} emissions from residential combustion, 2005–2019

Implications for air quality concentrations and trends

Authors

David Simpson¹, Jeroen Kuenen², Hilde Fagerli¹, Daniel Heinesen¹, Anna Benedictow¹, Hugo Denier van der Gon², Antoon Visschedijk², Zbigniew Klimont³, Wenche Aas⁴, Yong Lin⁴, Karl Espen Yttri⁴, Ville-Veikko Paunu⁵

¹Norwegian Meteorological Institute, Norway

²TNO, The Netherlands

³International Institute for Applied Systems Analysis (IIASA), Austria

⁴NILU-Norwegian Institute for Air Research, Norway

⁵Finnish Environment Institute SYKE, Finland

Contents

Authors and affiliations	2
Summary	4
1. Introduction	6
2. Gas-Particle partitioning	9
3. Emissions	11
3.1 Development of new emission Ref2_v2.1	11
3.2 Fuel consumption and fleet of appliances	11
3.3 Emission factors	15
3.4 Resulting emissions	18
3.5 Comparison with Nordic WelfAir	23
4. Model setup	25
4.1 Non-volatile POA setup	26
4.2 VBS setup	26
4.3 Residential wood-combustion emissions	29
4.4 Levoglucosan	29
5. Measurements	31
6. Comparison of modelled versus observed concentrations and trends	33
6.1 The winter 2017/2018 campaign	33
6.2 Modelled versus observed trends	36
7. Policy implications	43
7.1 Impacts on PM2.5	43
7.2 Source-receptor calculations	44
8. Conclusions	47
9. Acknowledgements	50
10. References	51
Appendix	56

This publication is also available online in a web-accessible version at <https://pub.norden.org/temanord2022-540>.

Summary

Condensable primary organic aerosol (CPOA) emissions are a class of organic compounds that are vapour phase at stack conditions, but which can undergo both condensation and evaporation processes as the stack air is cooled and diluted upon discharge into ambient air. Emission factors may misrepresent, and even miss, the amount of particulate matter (PM) or gas that actually enters the atmosphere, depending on the emission measurement techniques used. In the current emission reporting to EMEP/CLRTAP there is no clear definition of whether condensable organics are included or not, and, if included, to what extent.

In this study, new residential combustion emission estimates have been made for the years 2005-2019 (called TNO Ref2_v2.1) in a consistent manner, with improved estimation of fuel consumption (in particular wood) and emission factors, as well as an updated split of fuel use over different appliances and technologies. For these two elements, data were taken primarily from the Eurostat fuel statistics and the IIASA GAINS model. Three scenarios have been defined: a "typical" case, which is our best estimate, an alternative "ideal" case which excludes the impact of "bad combustion", and a "high EF" scenario in which higher emission factors are assumed than in the typical scenario. Total emissions in the typical scenario are around 40% higher than in the ideal case (in 2019), whereas resulting emissions in the "high EF" scenario are around 90% higher than in the typical scenario.

The Ref2_v2.1 inventory was used in a series of modelling studies which aimed to assess the importance of condensable organics for current air quality, for trends over time (2010–2019), and for source-receptor calculations.

Including condensables in a consistent way for all countries gave model results (concentrations, trends and bias) in better agreement with observations for OC and PM_{2.5} than when using the EMEP emissions which have condensables for some countries but not others. However, the model results were sensitive to the choice of Ref2_v2.1 scenario, and also to the assumptions concerning volatility of the CPOA emissions, and assumptions about extra intermediate-volatility volatile organic compounds (IVOC) associated with such emissions.

No single setup performed best for each site. There are many factors that can contribute to such mixed results (activity data, emissions factors, assumed combustion conditions, large and small scale spatial distributions issues in emissions, dispersion and CPOA/IVOC assumptions in the modelling), and much further work (and with other observational data-sets) will be needed to disentangle the reasons for model-measurement discrepancies, and to draw conclusions on how realistic the new emissions are.

Assumptions about volatility seem to be important for both the country-to-itself contribution, and for impacts of each country on others. In the few cases investigated so far, assuming inert CPOA provides results which generally lie within the range of the more complex VBS scenarios. Given the many uncertainties associated with the emissions and the modelling of POA and SOA, these results indicates that the inert CPOA assumptions provide a reasonable first approach for

handling POA emissions, which can hopefully be improved once our understanding of the sources and processing of these compounds improves.

The new emission data-base, combined with increasing availability of measurements of organic and other components, should provide the best available basis for future improvements in both the emission inventories and model formulations. Much analysis and further tests remain, both with the other model setups, and ideally with alternative secondary organic aerosol schemes to get a better idea of the sensitivity of the results to the various assumptions concerning both emissions and atmospheric processing of POA.

1. Introduction

Primary particulate matter (PPM) is composed of directly emitted particle mass plus any material that condenses into the particle phase shortly after initial release without undergoing chemical reactions. As will be discussed in more detail below, estimation of emission factors (EFs) for such emissions are also impacted by evaporation of some of the compounds before or after the point at which the EFs are estimated. PPM can also be divided into so-called filterable (solid) PM, denoted FPM, and condensable compounds, denoted CPM. The FPM fraction includes soot/black carbon (BC), ash, organic and other compounds. The CPM fraction includes inorganic compounds (mostly sulphates from sulphur present in fuels) and condensable organic compounds. The relation between total PPM emissions and the FPM and CPM is often written:

$$\text{PPM} = \text{FPM} + \text{CPM} \quad [1]$$

This report focuses on the organic components of PPM, and in analogy with (1) we can write:

$$\text{POA} = \text{FPOA} + \text{CPOA} \quad [2]$$

where POA is the total emission of primary organic aerosol compounds, and FPOA and CPOA are the filterable and condensable fractions of these. These condensable primary organic aerosol emissions are a class of semi-volatile organic compounds (loosely referred to as SVOC). The condensation and evaporation processes for these CPOA compounds are discussed further in Sect. 2, but a consequence is that emission factors measured in or close to the high-temperature high-concentration exhaust stack or pipe may misrepresent, and even miss, the amount of particulate matter or gas that actually enters the atmosphere; results are strongly dependent on the filters, dilution and sampling conditions of the emission measurement. Such issues were first highlighted in the US by Donahue et al (2006) and Robinson et al (2007), and Robinson et al (2010) give a very clear overview of condensable organics. Further information (with a more European focus) can be found in Nussbaumer et al (2008a,b), Denier van der Gon et al. (2015) and Simpson et al. (2020).

Denier van der Gon et al. (2015), of the Dutch TNO institute, highlighted the importance of CPOA for European air quality in general. They pointed out that in the current emission reporting to the European Monitoring and Evaluation Programme (EMEP, www.emep.int), as part of the Air Convention (<https://unece.org/environment-policy/air>), there is no clear definition of whether condensable organics are included or not, and, if included, to what extent. Denier van der Gon et al. (2015) constructed a new emission inventory for Europe, in which CPOA were consistently included, and found significant differences between this resulting top-down inventory and the national inventories. For some countries, which were known to include CPOA in their national inventories (e.g. Norway), the so-called TNO-newRWC emissions were rather similar to the national estimate, whereas for other countries,

which were known to exclude CPOA (e.g. Sweden at the time, or Germany) the TNO-newRWC emissions were higher by up to a factor 3–4. Overall the TNO-newRWC emissions resulted in factor 2–3 differences for many countries. Modelling simulations with the revised inventory showed a substantially improved agreement between measured and predicted organic aerosols. These comparisons strongly suggested that primary aerosol (PM) inventories needed to be revised to include the CPOA components of PM.

In March 2020, the Meteorological Synthesizing Centre – West of EMEP (EMEP MSC-W, see www.emep.in/mscw) hosted an expert workshop on condensable organics (funded by the Nordic Council of Ministers, NMR), which led to the overview document published as Simpson et al. (2020). This workshop brought together experts in emissions, measurements, inventories, and policy from Europe and North America, and created a much better understanding of the issues and possible approaches for dealing with this important class of compounds. Discussions at the workshop confirmed that even when countries did include condensables, there were significant differences in the methodologies used. Furthermore, the workshop agreed that, as a first step, use of the latest (now called “Ref2”) TNO emissions for residential small combustion (where condensables are added to small-combustion emissions in a harmonised way) is a good first no-regret step for describing condensable emissions in atmospheric dispersion modelling.

Emissions reporting in Europe uses the so-called ‘GNFR’ system (e.g. Matthews et al., 2021), and emissions from small combustion system such as residential wood burning (RWC) or domestic coal fires are entered into GNFR sector C (“small combustion”). After discussions within the EMEP Bureaux and elsewhere, EMEP MSC-W model calculations in 2020 were conducted in which all GNFR C emissions were replaced by TNO Ref2 emissions for this sector in order to produce more consistent model results across the EMEP domain (Denier van der Gon et al., 2020, Fagerli et al., 2020). Further discussions between TNO, the EMEP Centre for Emissions Inventories and Projections (www.ceip.at) and parties to the Air Convention led to the model calculations in 2021 using the so-called EMEPwREF2.1C emissions, in which national emissions were retained for countries which were believed to already include condensables, but TNO Ref2.1 GNFR C emissions were used for the remaining countries (Matthews et al., 2021, Fagerli et al., 2021). These model results, and in addition model results using officially reported PM emissions, were compared to EMEP and European Environment Agency observations - and showed improved performance for PM_{2,5}, especially in wintertime, in the case where condensables were consistently included. The improvement was seen for most countries, although as expected, the extent of the change depends on the country and location (and the methods used to define PM emissions in nearby countries). Although there is good evidence for the basic concepts which were applied, many of the assumptions were recognised as being very uncertain.

A major part of the current work (Sect. 3) has been to prepare new emission inventories, with condensables treated in a consistent way, over the time-period 2005–2019. We then use a combination of modelling (Sect. 4) and measurements (Sect. 5) to investigate the consistency of the new emissions time-series with observations (Sect. 6), and with our ability to simulate these time-series and their trends with the EMEP MSC-W model. Finally, we show calculations of source receptor matrices (Sect. 7) for a few countries, and discuss some of the policy consequences of the revised emission estimates.

2. Gas-Particle partitioning

The impacts of temperature and concentration on EFs for semi-volatile compounds can be explained by simple gas-particle absorption-partitioning theory (Pankow, 1994, Donahue et al., 2006), which suggests that:

$$\frac{C_{i, (pm)}}{C_{i, (g)}} = \frac{C_{om}}{C_i^*} \quad \text{Eqn [3]}$$

Where $C_{i, (pm)}$ and $C_{i, (g)}$ are the concentrations ($\mu\text{g}/\text{m}^3$) of compound (i) in the particle and gas phase, respectively, C_{om} is the concentration of the total organic particulate matter (ie sum of all organic compounds, $\mu\text{g}/\text{m}^3$), and C_i^* ($\mu\text{g}/\text{m}^3$) is the effective saturation concentration (related to vapour pressure). Importantly, the C_i^* term is very temperature sensitive; the higher the temperature the higher the saturated vapour pressure, the more evaporation, and thus (from Eqn. [3]) the higher the proportion of compound *i* in the gas-phase. As temperatures drops, C_i^* is reduced, and gas-phase compounds increasingly condense into the particle phase. In the ambient atmosphere, the C_{om} term is simply the total concentration of all the organic compounds (and is often denoted simply as organic matter or aerosol, OM or OA), and Eqn [3] shows that the more polluted an air mass is the higher the proportion of the semi-volatile organic compounds (SVOC) in the particle phase. Equation [3] is used in chemical transport models for both primary and secondary organic aerosol components, through the so called volatility basis set (VBS); this will be discussed further in Sect. 4.2.

Concerning POA, Figure 1 is a highly simplified sketch of the main processes associated with the evolution of POA emissions. Phase (A) represents a location very close to the combustion itself, and here the temperature (and hence each C_i^*) is often so high that very little or no SVOC (using the term loosely here, see Sect. 4.2) are present on the solid core – this core is represented by the grey circle, and is equivalent to the FPOA in Eqn. [2]. In the first few seconds after this combustion the stack gases cool down, C_i^* is reduced, and some of the emitted SVOC (which surround in the core in very high concentrations) can condense onto the solid core, giving a substantially higher mass in the particle phase (these condensed SVOC are shown as the dark green circle in Fig. 1), with a maximum contribution reached at phase (B). The next major process occurs as the stack exhaust is diluted with ambient air, which corresponds to a change of C_{om} from possibly 1000s of $\mu\text{g}/\text{m}^3$ to ambient C_{om} levels of perhaps 1–10 $\mu\text{g}/\text{m}^3$. This dilution also occurs very quickly, and equilibrium drives SVOC from the condensed phase into the now much diluted vapour phase – moving from phase B to C in Fig. 1. As the plume dilutes further in the atmosphere and is transported downwind (phases D, E) the particle phase can accumulate secondary organic aerosol (SOA) - compounds which are formed in the atmosphere following reaction of volatile organic compounds (VOC, including gaseous CPOA) with oxidants such as OH, O₃ and NO₃.

The emission factors (EFs) used in inventories are derived in multiple ways, and the values found depend on the EF measurement device, burning conditions, wood-load, humidity, etc. In terms of Fig.1 these EFs are usually derived at some point between

(B) and (C), that is after the point of maximum organic loading, but before ambient conditions are achieved. The interpretation of these EFs is non-trivial, and some interaction is needed between modellers who make use of the emissions and the emissions providers, so that all parties understand the definitions and characteristics of the EFs and associated POA emissions. These processes are explained in greater detail in Donahue et al. (2006) and Robinson et al. (2010).

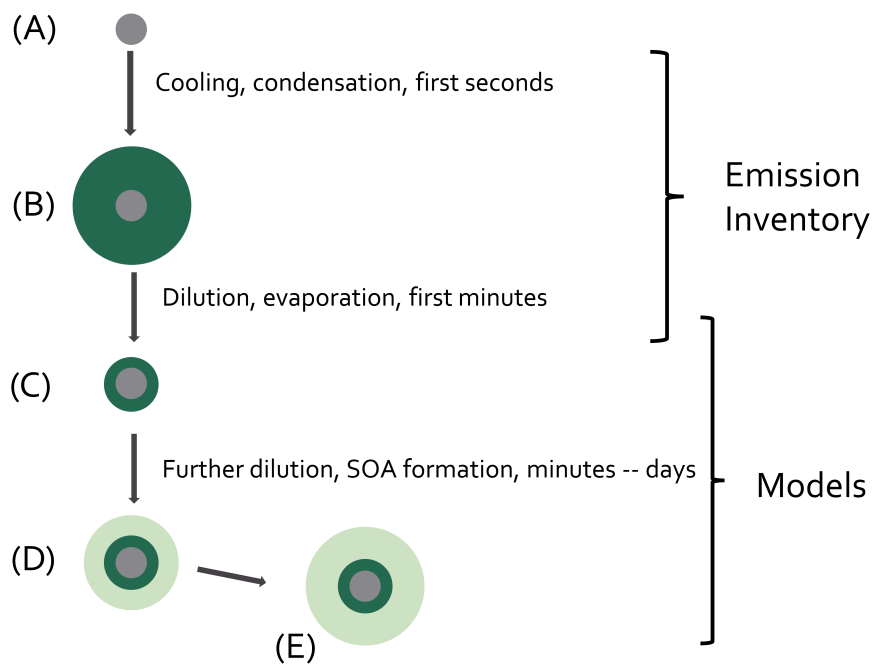


Figure 1. Sketch showing the development of POA from stage (A) in the combustion area to stage (E) far downwind. See Sect. 2 for details.

3. Emissions

3.1 Development of new emission Ref2_v2.1

Consistency and completeness of emissions over the study domain is an important first step to assess the impact that PM emissions have on the environment. Given the inconsistencies in current reporting of PM in emission inventories by Parties to the Air Convention (see Section 1), a new state-of-the-art bottom-up emission inventory is necessary to ensure consistency in the baseline emissions. This new bottom-up inventory in this study essentially comprises a major update of Denier van der Gon et al. (2015), taking into account the most up-to-date information from various sources including scientific emission literature, but also data exchange and harmonisation with IIASA-GAINS (IIASA, 2021, Klimont et al. 2017) and other European-wide data sources with information on fuel wood consumption, fleet structure, emission factors, etc.

The domain of this study is UNECE-Europe, with emissions estimated for 42 individual countries. At the Eastern side of the domain, emissions for Turkey, Ukraine and the European part of the Russian Federation are included. For each country, emissions of particulate matter (PM_{2.5} and PM₁₀) from solid fuel combustion in small combustion appliances were estimated, including coal, wood and wood pellets. For each year in the period 2005–2019, fuel consumption and appliance type data were collected and processed into a consistent dataset. A set of emission factors was derived, distinguishing fuel and appliance type, several modes of operation, and two fuel moisture contents. The emission factors are defined solely based on technical appliance characteristics and fuel specification, and differentiate between the main components of PM (elemental carbon, organic carbon and non-carbonaceous components) and segregate the filterable and condensable part of organic particulate matter (FPOA and CPOA, respectively).

3.2 Fuel consumption and fleet of appliances

Activity data (solid biomass and solid fossil fuel consumption in households) are primarily taken from official energy balances for each country, as available from the Eurostat energy statistics (Eurostat, 2021). The quality of Eurostat data has been continuously improved over the last decades, based on among others past local and regional research projects aimed at gaining a better insight into actual household use of biofuels and other renewable energy sources. In general this led to an increase in the estimated wood usage. For biofuels in particular, Eurostat data were nevertheless cross checked against other sources of data, including country reports on emissions of greenhouse gases and air pollutants, and fuel consumption data from the GAINS model (IIASA, 2021, Klimont et al. 2017), including latest estimates from the IIASA team being part of this project. Also an independent FAO report (UN FAO, 2017) that builds on the results of an extensive global survey has been used. These comparisons are necessary because especially for biomass combustion, statistical data may still not represent the actual consumption, as fuel wood for domestic use is partly harvested or collected outside of any administration, and may therefore be partly lacking in statistical data.

From these comparisons, some updates to the Eurostat fuel consumption were made, especially in Eastern European (mostly non-EU) countries, where data from alternative sources (in particular the GAINS model) were used instead. In spite of this our best estimate of the actual consumption of wood in several eastern European countries remains relatively uncertain. In some cases there is very little information to base estimates on.

In order to understand discrepancies between countries, we have analysed wood consumption data per capita and per heating degree day (HDD, averaged per country) as shown in Figure 2. The Figure suggests strong variations between countries. Most of these differences are explainable by differences in the availability and price of fossil heating fuels, in addition to the availability of distribution networks and local or national regulations regarding wood use. Also the local and regional availability of wood from forested areas seems to play an important role. Another cause for discrepancies between countries may however lie in underestimation of actual wood use in certain country estimates, especially for non-EU countries. However, in the absence of any other published data that could be used as an alternative, no further increase in wood consumption over either Eurostat, GAINS or FAO data was proposed at this stage.

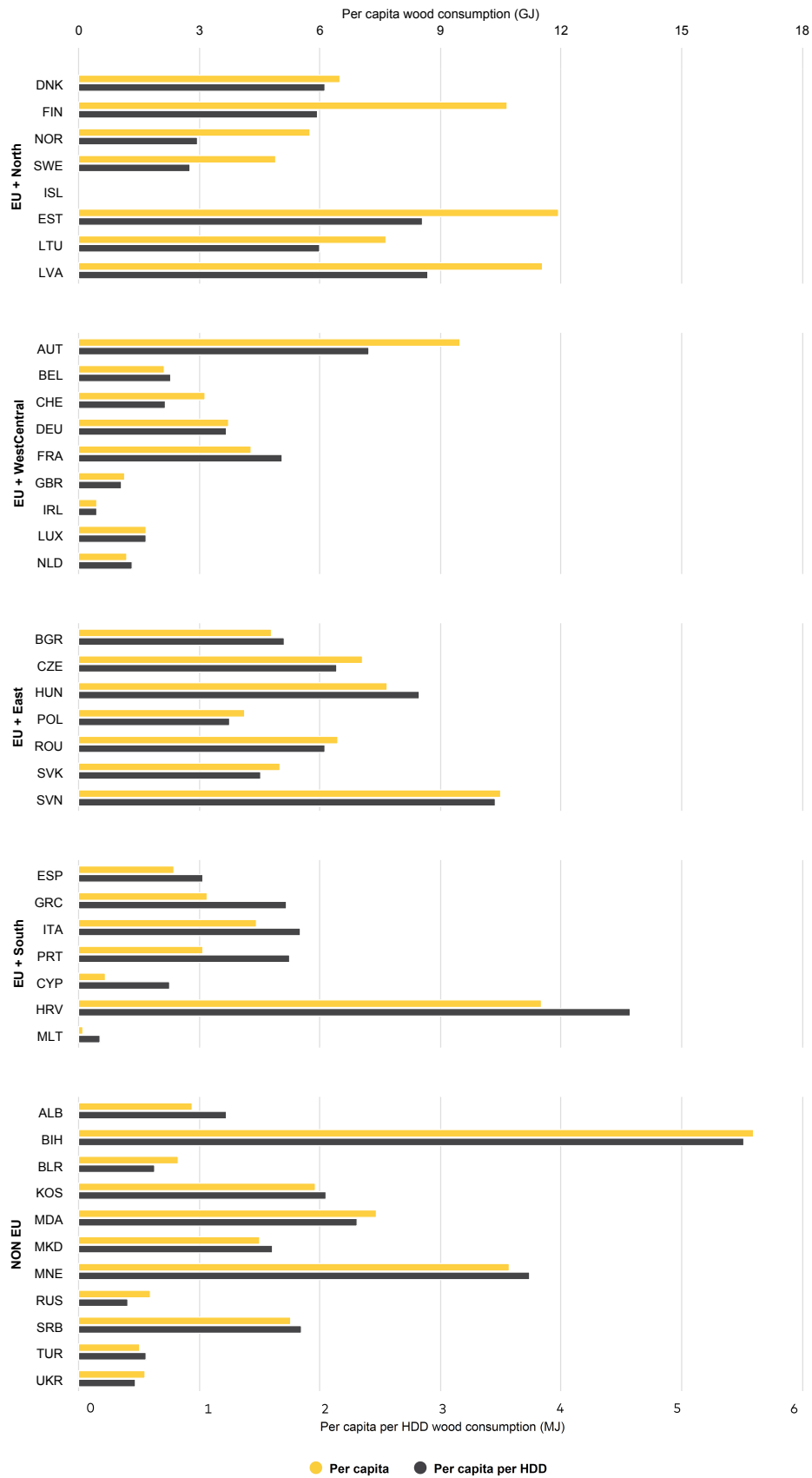


Figure 2. Wood consumption (this study) expressed per capita and per heating degree day.

Note: Bars not shown for some countries due to low values

Figure 3 shows the resulting total annual consumption of solid fuels in Europe for 2005 to 2019. The figure indicates that solid fuel use as a whole has increased between 2005–2010, after which coal use decreased again, whereas wood use remained relatively constant from 2010 onwards. Interannual variations are mostly related to climatological differences (cold vs. mild winters).

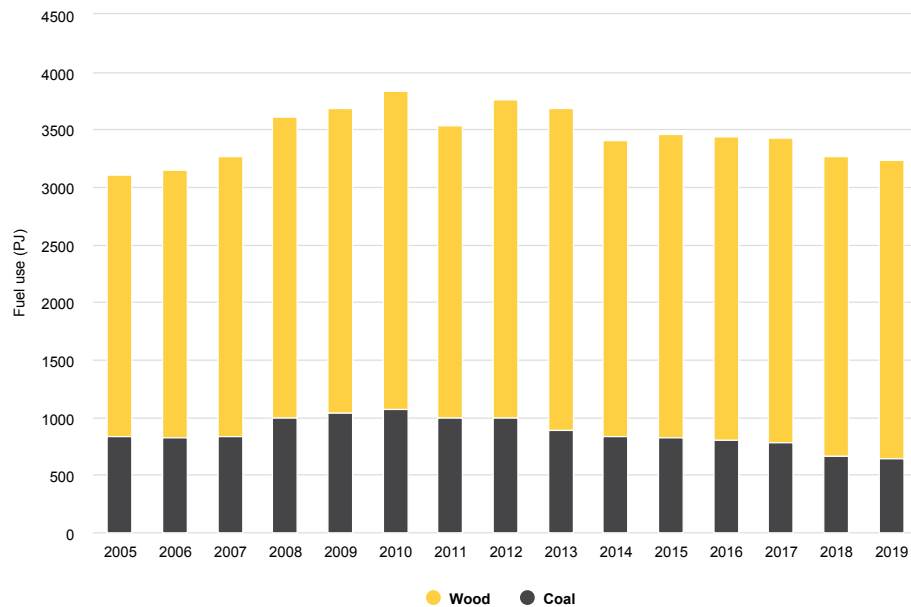


Figure 3. Residential solid fuel consumption in Europe per year.

The split of the fuel use over different appliances was primarily adopted from the IIASA GAINS model (IIASA, 2021), in close consultation with the team at IIASA. The GAINS data differentiate between main appliances (e.g. boilers and stoves), fuel types (e.g. traditional wood logs and pellets) and also between technology levels and environmental standard (e.g. traditional vs. improved vs. modern stoves). One major change was made for France, where IIASA data suggested that all traditional stoves in France would have been entirely replaced by 2015 with new stoves, in contrast to other countries where the typical share of traditional stoves in 2020 would be close to 20% as minimum, hence the data for France appear overly optimistic and not representative given the use of these appliances especially in rural areas. Therefore the split for France was updated to the split for Germany (a conservative approach, since Germany is a country where typically the environmental standards are more stringent than in many other countries), implying around 20% traditional stoves remaining in 2020.

Figure 4 presents the estimated overall split of the total European wood consumption over the different appliance types, for selected years in the considered time period. It shows that the shares are varying with time. Within the category of heating stoves, the average share of traditional stoves (which accounts for 40% of wood consumption in 2005) decreased to 28% in 2019. On the other hand, shares of modern stoves and automatic boilers (mostly pellet boilers) are gradually increasing. Figure 4 suggests however that the pace at which the renewal of the appliance fleet proceeds in Europe may not be considered particularly high, as overall only around

30% of the old stoves present in 2005 is replaced in a 14-year time span. Compared to for instance road vehicles (for which fleet renewal occurs much faster), most wood burning equipment apparently have a much longer lifetime.

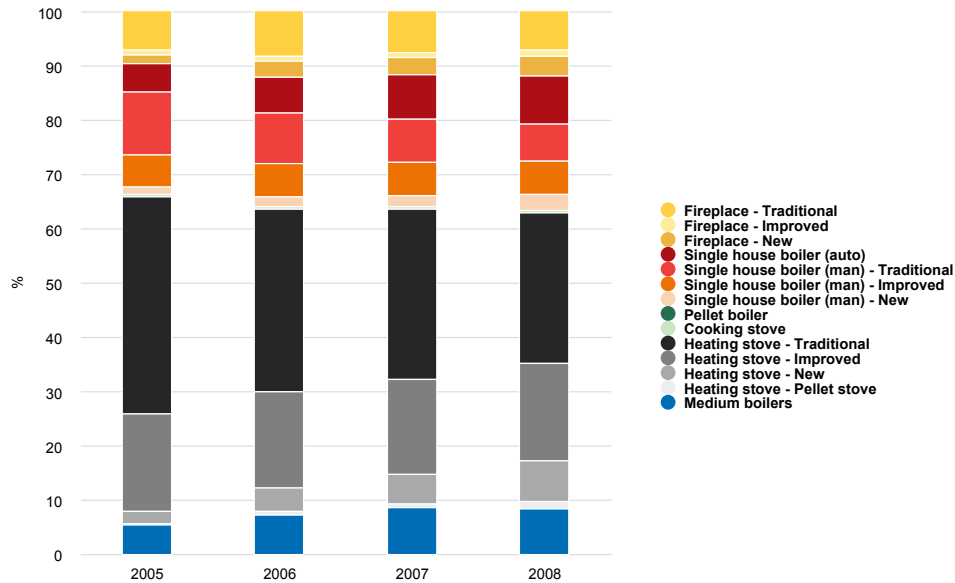


Figure 4. European average wood consumption split over appliances and technologies in different years.

3.3 Emission factors

Emission factors for wood combustion were determined based on a literature survey. Multiple emission factors were identified for each relevant appliance type, as is illustrated by Figure 5 (note the logarithmic Y-axis). The figure shows that despite selecting only emission factors that include the condensable component of PM and represent actual real-world emissions, for any given class of appliances a large range is found, not only as shown by the range bars, but also in the central values (blue points). This is typical when measuring particulate matter emission from small wood combustion appliances, even between those of comparable design and environmental standard. For most appliance classes emission factors appear to vary by around an order of magnitude. In general the range bars in the figure indicate the range that was measured throughout different phases of the combustion cycle. The variation in the central values (blue dots) are likely related to apparently random differences in local circumstances during the measurements, including performance of the appliance, variation in the used start-up and shut down routines, fuel characteristics/quality (wood type, piece size and moisture content), load factors and other factors influencing combustion efficiency. Figure 5 shows two lines, the red line representing the arithmetic (not geometric) average of the central values per equipment class, and the green line the median. Given the big variation of the emission factors and the relatively larger number of available observations, the median values are assumed to be the most representative. The green line shows that the median emission factor consistently decreases with environmental standard, with the emission of a traditional stove being more than a factor of 20 higher than a

modern pellet boiler. In addition, with the possible exception of pellet stoves, all appliance types appear to be highly sensitive to suboptimal user operation and fuel characteristics.

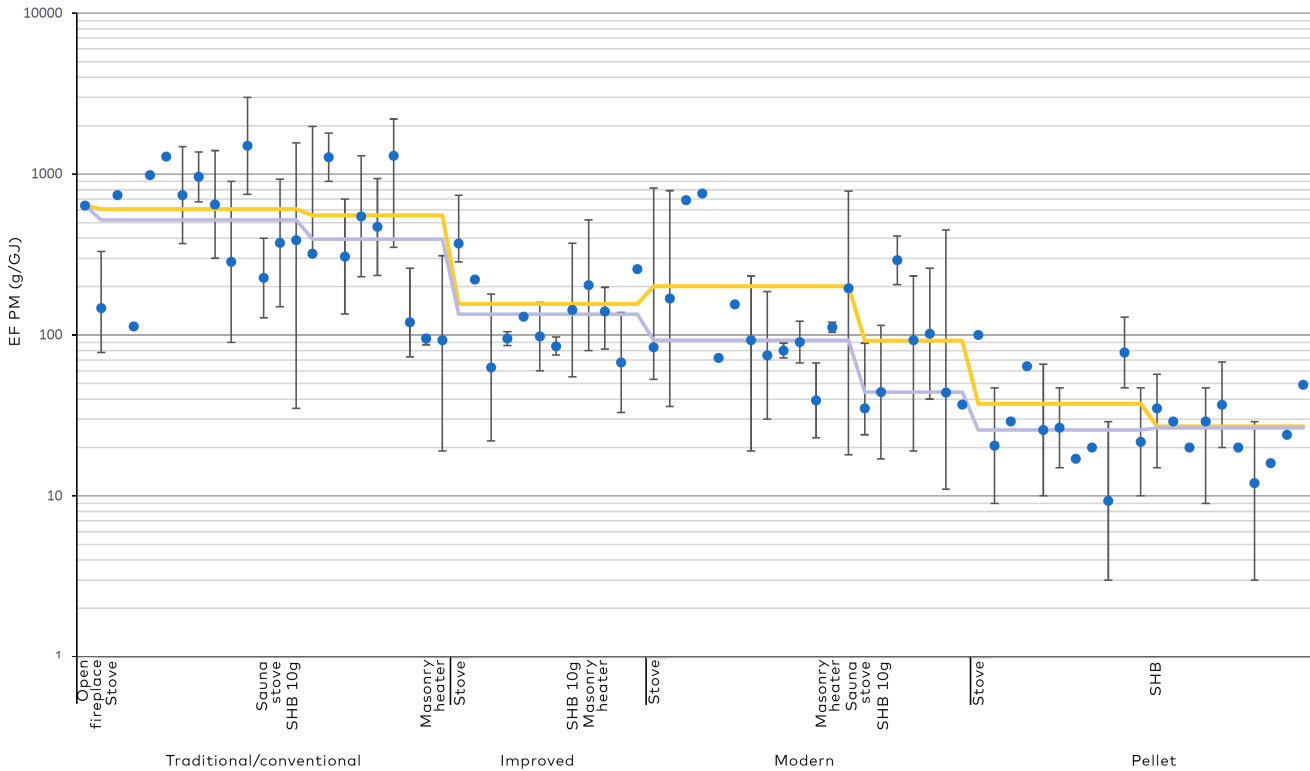


Figure 5. Emission factors collected for wood consumption from various appliance and technology types.

For coal combustion emission factors were primarily taken from an assessment of the available information in the GAINS model, complemented by information from the scientific literature.

PM emissions from small combustion also depend on the way the device is operated. Depending on the appliance type and the way it is managed, excess emissions of up to a factor 5 may occur. In this study, two user impact elements were specifically addressed:

1. The use of wood that is not well dried
2. Partial load of the combustion chamber

These effects are considered especially important for small appliances which may be operated by inexperienced users. Therefore, for fireplaces, heating stoves and small boilers these non-ideal combustion conditions are assumed to occur in a limited number of cases, where for larger appliances it is assumed that these non-ideal conditions do not occur. An estimate for the impact of both the use of insufficiently dried wood and partial load of the appliance on the emission factor of each

appliance type was made. In addition an estimate was made of the incidence of these conditions. These two estimates were then combined to calculate the overall influence on emissions and define a new set of adjusted emission factors, which are considered more representative for the real-world situation.

Resulting emission factors including partial "bad combustion" are shown in Table 1, which also includes the factors without this adjustment (between brackets) for comparison. An important observation from these results is that the effect that "bad combustion" may have on emissions is in a relative sense stronger for the more modern types of stoves and boilers. This implies that part of the improved environmental performance of more modern stoves may be offset by user behaviour. On average, the impact on stoves is found to be more significant than for boilers. These results should be used with caution however, as both the impact of "bad combustion" as well as the share at which this happens are highly uncertain.

Table 1. Typical emission factors for residential wood burning for the most important categories, taking into account "bad combustion" impact (EF without this effect shown in brackets).

Technology	Heating stove	Single house (small) boiler
Traditional	776 (519)	552 (395)
Improved	361 (192)	238 (158)
Modern	194 (103)	119 (79)
Pellet	31 (26)	42 (35)
Pellet + ESP	5 (4)	4 (4)

The emission factors with and without the impacts from "bad combustion" have for this study been taken as two different scenarios, where the case without the user impact is referred to as the ideal scenario and the other case is referred to as the typical scenario. In addition to the typical and ideal scenario, a third scenario has been defined, which is different from the typical scenario by selecting not the median value of the emission factors (see Figure 5) but the median of the top-5 of the literature emission factors (in case less than 10 values were reported, top-3 is used instead). This hypothetical scenario should be regarded as an indication for what emissions could be if the higher emission factors from literature would be more representative for the sector as a whole. The overview of emission scenarios is provided in Table 2, and also includes the labels used for the modelling work of Sect. 5.

Table 2. Overview of scenarios defined for this study

Scenario	Emission factor	"Bad combustion"	Label for modelling
Typical	Median of full range of emission factors from literature survey	Included	C (central EF)
Ideal	Median of full range of emission factors from literature survey	Excluded	L (low EF)
HighEF	Median of top-5 (or top-3) of emission factors from literature survey	Included	H (high EF)

3.4 Resulting emissions

Figure 6 shows the resulting PM_{2.5} emissions for 2005–2019, differentiated to groups of countries. It shows a small increase in emissions in the period 2005–2010, followed by a decrease in the period 2010–2019. The decrease over the entire period 2005–2019 amounts to 1.2% per year on average, however when the period 2010–2019 is selected the decrease amounts to 2.6% per year on average.

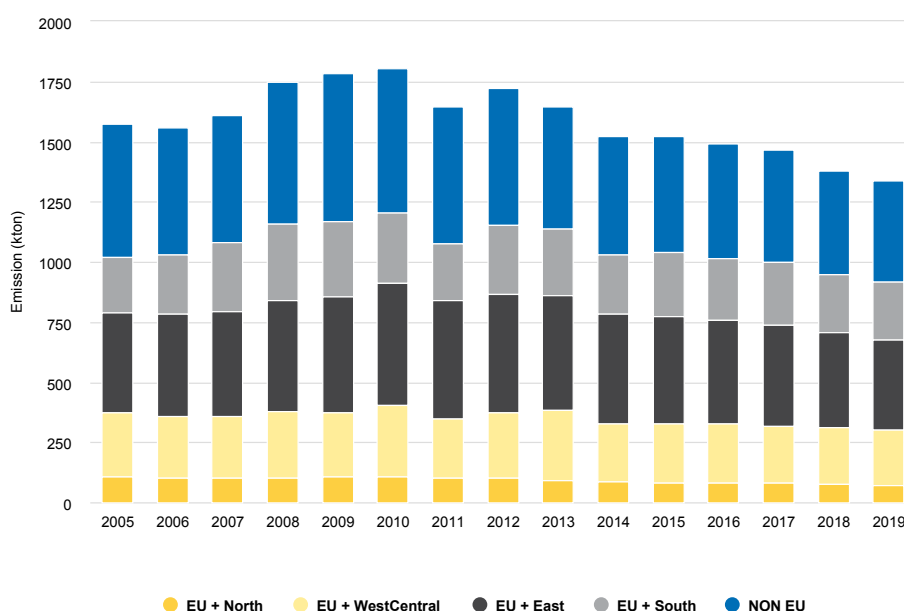


Figure 6. Resulting PM_{2.5} emissions per country group in Europe, from 2005–2019, including condensables, for the typical scenario.

Figure 7 shows resulting PM_{2.5} emissions for the 3 scenarios for each country for the year 2018 as an example. In the EU+ countries (= EU27 + Norway, Iceland, Switzerland, UK), Poland has the highest emissions which can be explained by the high share of both wood and coal in the energy mix for residential heating.

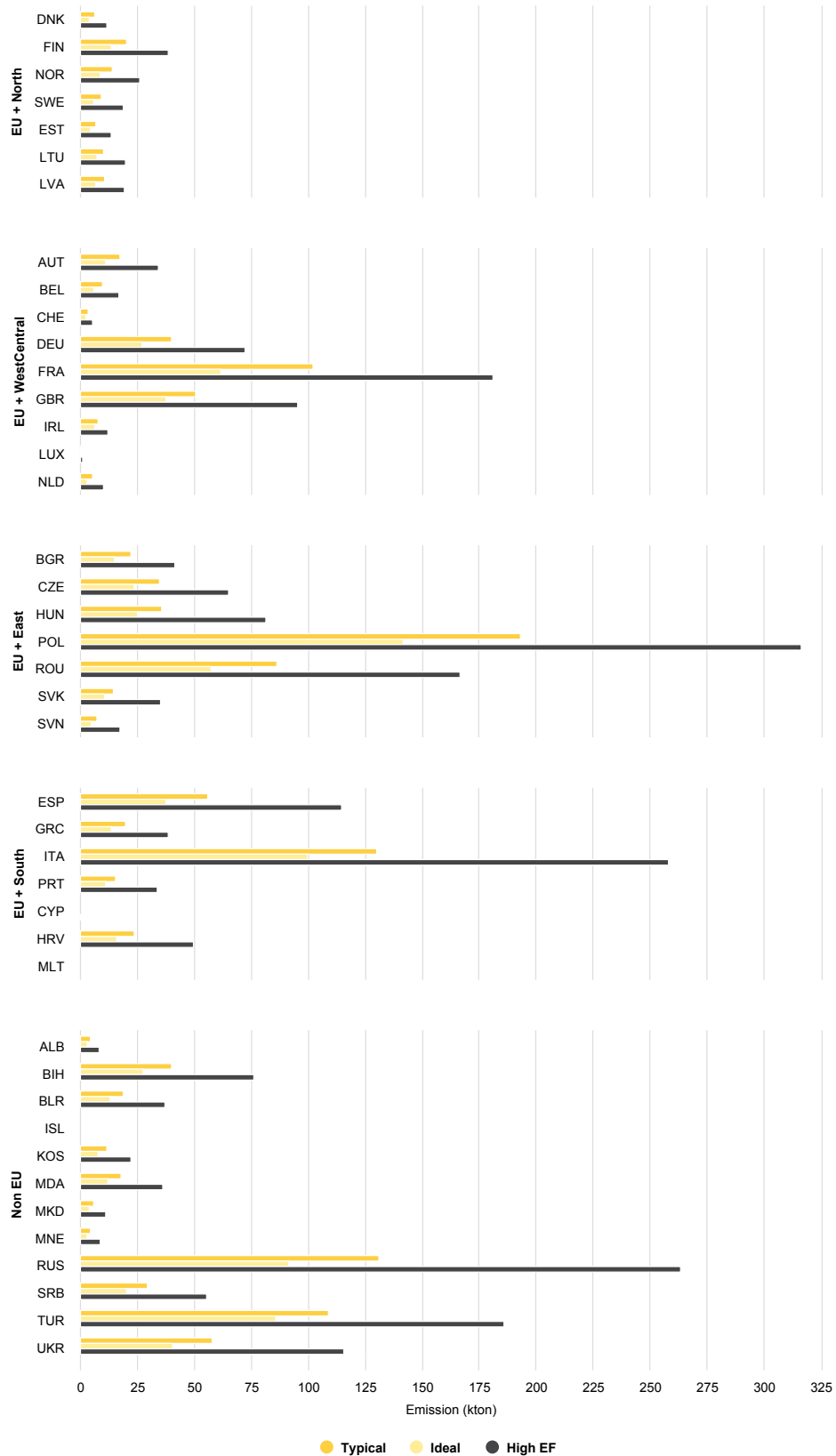


Figure 7. PM_{2.5} emissions by country for the 3 scenarios (Typical, Ideal and HighEF) for the year 2018.

Note: Bars not shown for some countries due to low values

To illustrate the importance of specific appliances and fuels to emissions, Figure 8 shows again the emissions for the 3 scenarios, but now for all 42 countries together, for the years 2005 and 2019. The figure shows that in all 3 scenarios, heating stoves using wood dominate the emissions, followed by small boilers using wood and heating stoves using coal. The share of coal in emissions has decreased. Overall emissions decreased in all 3 scenarios on average by around 15% between 2005 and 2019 (which was also shown in Figure 6).

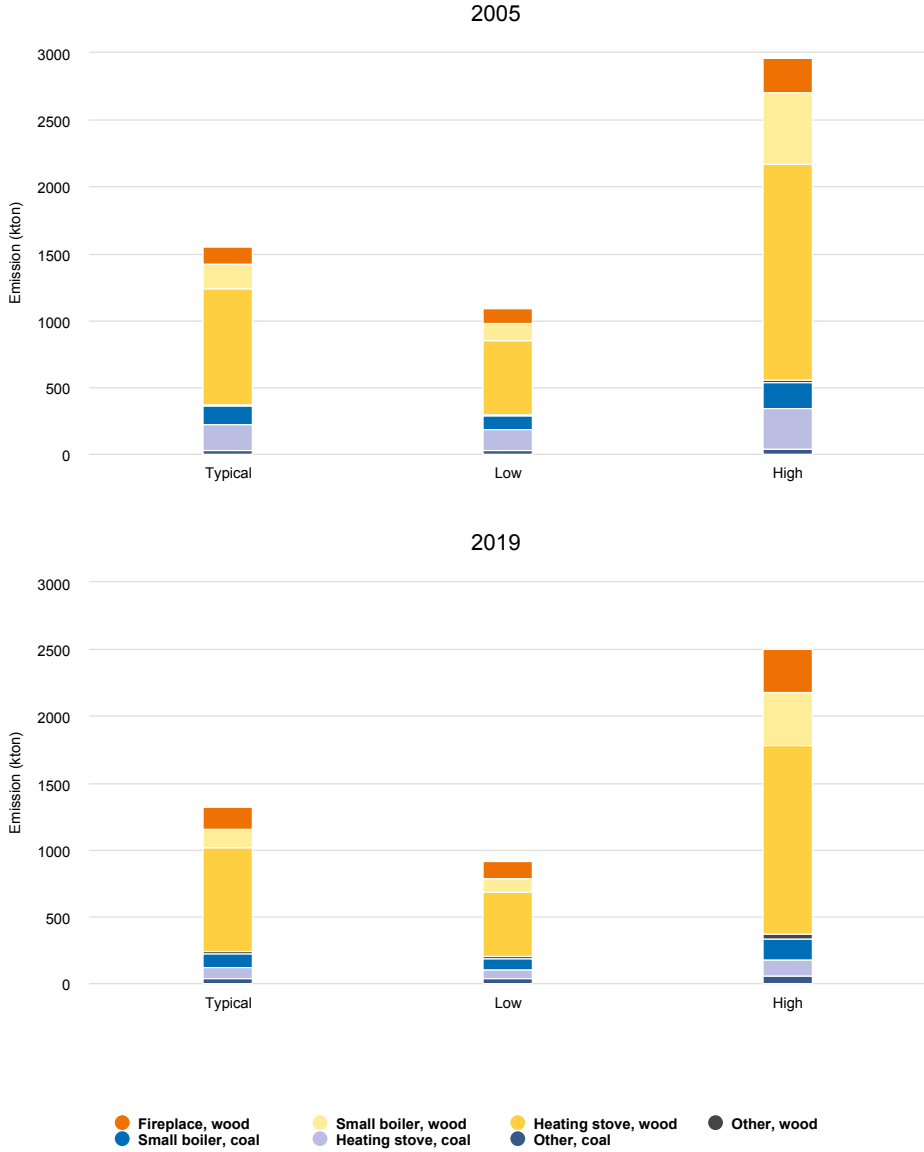


Figure 8. PM_{2.5} emissions by fuel (coal and wood) and appliance type for the years 2005 and 2019, for each of the 3 scenarios.

An interesting comparison is how these consistently calculated emissions compare to the national reported emission inventories to CLRTAP. Therefore, Figure 9 shows a comparison between the Ref2 emissions and the CAMS-REG-v5.1 dataset (Kuenen et al., 2022) which developed on the basis of the official reported emissions (based on the 2020 inventory submissions). The figure shows a diverse picture, for some countries (e.g. Norway, Belgium, United Kingdom, Hungary, Spain, Croatia) the emissions in both datasets are rather similar, whereas for some other countries the Ref2_v2.1 emissions are significantly higher than the official reported emissions (e.g. Finland, Germany, France, Poland). To a large extent this is related to the exclusion of condensables in official inventories, but also country-specific issues may play a role (e.g. Finland has a rather different fleet type compared to the rest of Europe, for instance with wood-fired sauna stoves which are uncommon in the rest of Europe).

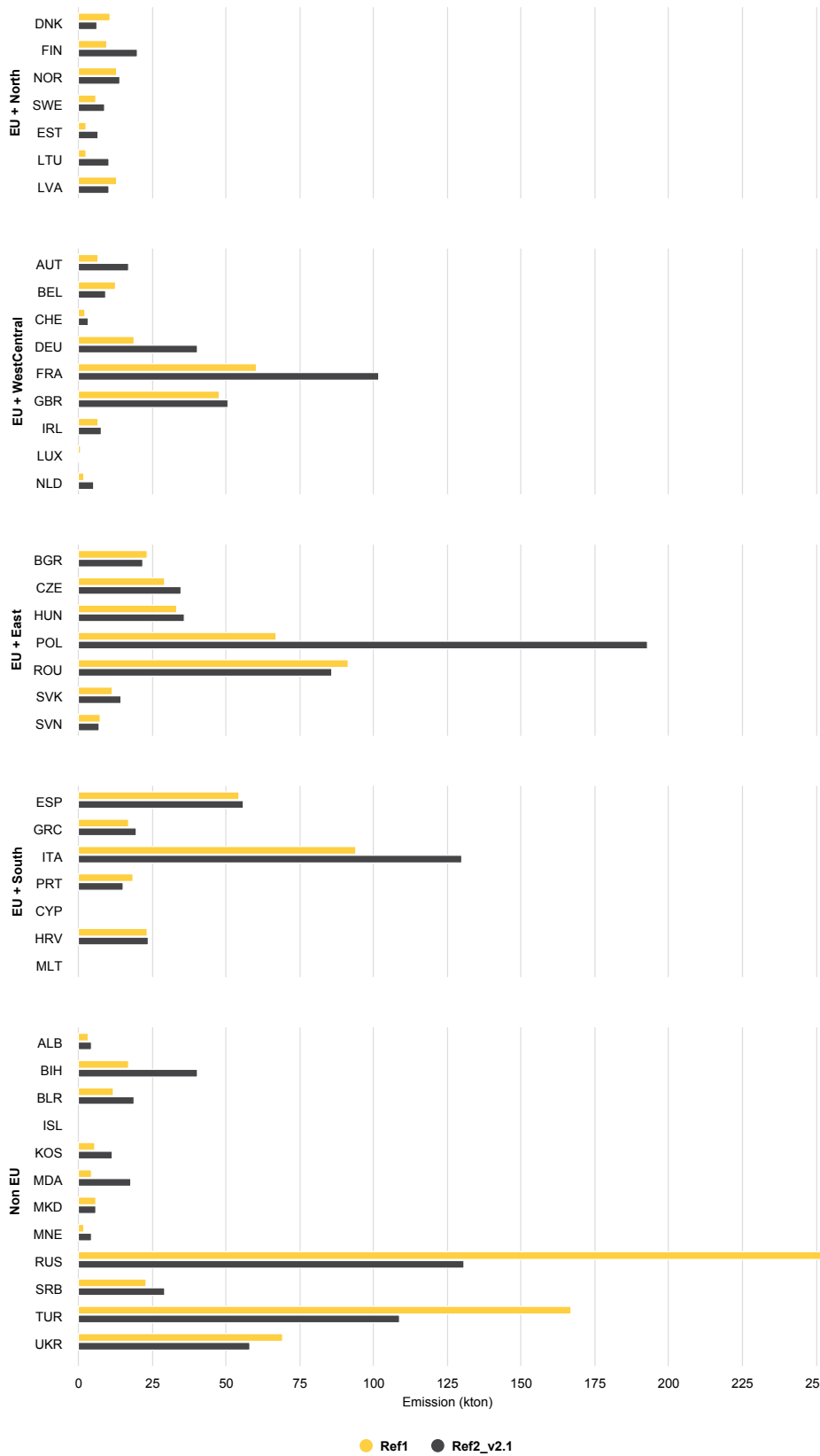


Figure 9. Emissions from this study (Ref2 v2.1) compared to official reported emissions, adapted from the 2018 CAMS-REG-v5.1 dataset, for EU+ countries (EU27 + UK, Norway, Switzerland).

Note: Bars not shown for some countries due to low values

The resulting emissions are spatially distributed across the European domain using the same approach as for the CAMS-REG-v5.1 emission inventory (which is a further development of the inventory described in Kuenen et al., 2022). This implies that emissions from coal combustion are spatially distributed using rural population as a proxy, oil & gas combustion are distributed using total population as a proxy and for wood combustion a dedicated proxy representative for wood use is used. This proxy takes into account rural population and also proximity to wood (to account for locally harvested wood), therefore largely excluding wood combustion in cities. More details can be found in Kuenen et al. (2022).

3.5 Comparison with Nordic WelfAir

The spatial distribution of $PM_{2.5}$ emissions in the Nordic countries was compared to a Nordic emission inventory developed in the NordicWelfAir-project (Paunu et al., 2021). The normalised spatial distribution of $PM_{2.5}$ emissions are presented in figure 10. To assess the similarity in the spatial distributions, index of agreement λ was calculated (Paunu et al., 2021). The results are presented in Table 3.

The index of agreement shows good agreement in Finland, reasonable agreement in Denmark, slightly lower in Sweden, and poor agreement in Norway. In Finland, the Nordic inventory had more emissions weighted to the rural areas, as opposed to the Ref2_v2.1, where the emissions are more concentrated to cities. In Denmark, in the Ref2_v2.1 inventory the continental Denmark has more weight than in the Nordic one, and the distribution around Oslo is different. In Sweden and Norway, the Ref2_v2.1 has a more even spread of emissions, especially in the rural and mountainous regions of Norway. The Nordic inventory has higher emission weight in Stockholm than the Ref2_v2.1, whereas the Ref2_v2.1 weights more emissions to the southernmost part of Sweden.

In general, the conclusions of Paunu et al. (2021) on comparison of the spatial distribution of the emissions between the Nordic inventory and TNO-newRWC hold here as well. The main differences are how the emissions are weighted between urban and rural areas. National characteristics play an important role here, as the Nordic inventory used national data and methods for the spatial distribution. One common method in the Ref2_v2.1 produces different results in different countries, as the Nordic inventory has more weight in rural areas than the Ref2_v2.1 in Finland, but less in Norway. The differences are likely mainly due to more detailed information on houses, especially their appliances and wood use in the Nordic inventory, which is hard to capture with proxies not based on national data. The national data also allows more detailed description on differences between urban and rural areas (including differences between different rural areas). The index of agreement was lower for Sweden and Norway in this comparison than in Paunu et al. This is partly due to updated Nordic inventory, but also the Ref2_v2.1 and TNO-newRWC have different spatial distributions. Possible future work would be to apply the spatial distribution from the Nordic inventory to the Ref2_v2.1 and assess how this would affect the modelled concentrations.

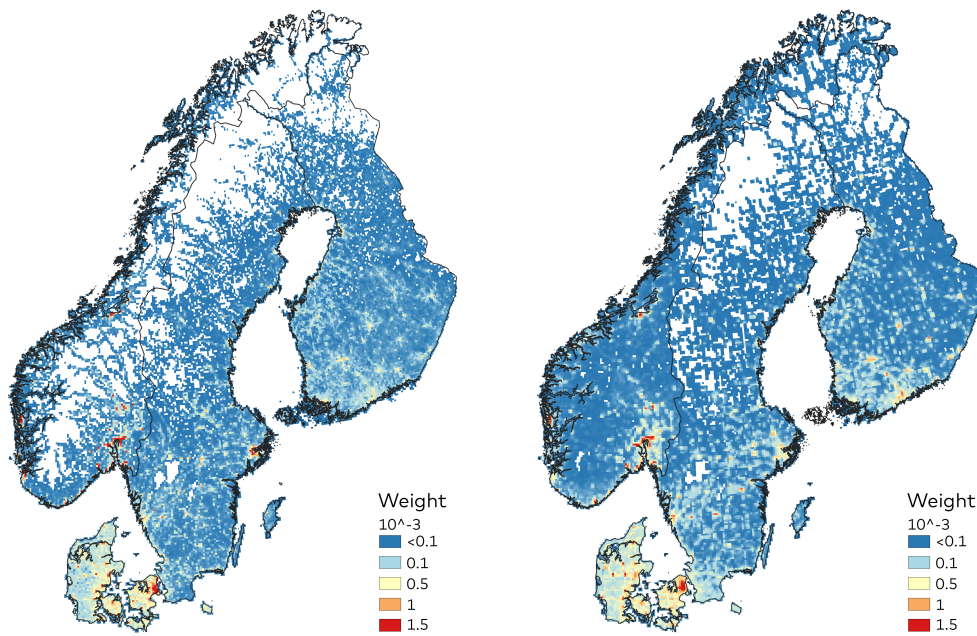


Figure 10. Normalized spatial distributions of $PM_{2.5}$ emissions from residential combustion in the NordicWelfAir-inventory (left), and from the new inventory produced in this project (right). Normalization of the emissions were done separately for each country.

Table 3. Index of agreement (λ) for the spatial distribution of $PM_{2.5}$ emissions of residential combustion between the Nordic and Ref2_v2.1 inventories.

Denmark	Finland	Norway	Sweden
0.73	0.78	0.59	0.68

4. Model setup

The EMEP MSC-W chemical transport model is a 3D-Eulerian model hosted at Met Norway (Simpson et al., 2012, 2021), whose main aim is to support governments in their efforts to design effective emissions control strategies in Europe (Amann et al., 2020). The model is primarily applied for European air quality studies (e.g. Denier van der Gon, 2015, Jonson et al., 2017), though also used at global scales to assess international pollution issues (e.g. Mills et al., 2018, McFiggans et al., 2019). The standard model has a variety of chemical schemes ranging from simpler carbon-bond approaches to complex (500-reaction) schemes, and has used a variety of methods for secondary aerosol simulation (Simpson et al., 2007, Bergström et al., 2012, McFiggans et al., 2019). The standard model uses meteorology from the European Centre for Medium Range Weather Forecasting Integrated Forecasting System (ECMWF-IFS).

In this work, we use the standard model setup for all sources, except for POA from RWC which is explored in more detail as described below. As noted in the introduction, primary POA emissions can be considered to be the sum of filterable POA (FPOA) and condensable POA (CPOA). The TNO emissions provided these two components separately, so the modelling studies focus on differences in the handling of the CPOA fraction.

The model setups used are summarised in Table 4, which combines a label for the type of volatility assumptions (NV, SV, SIV, explained below), and the TNO emission scenarios used (C, or H, c.f. Table 2). Also, for some runs we have used the high resolution 0.1x0.1° model setup, but those runs with "32" in the scenario label (e.g. NVC32) a 0.3x0.2° resolution was used.

The 'EMEP' setup represents the data as officially submitted to the Convention through EMEP Centre for Emissions Inventories and Projections (<https://www.ceip.at>). The "non-volatile" (NV) setups are discussed in Sect. 4.1, and the setups involving semivolatile POA and IVOC are discussed in Sect. 4.2.

Table 4. Model scenarios used in EMEP runs. (Default runs are 0.1x0.1° degree lon/lat, but suffix 32 runs use 0.3x0.2°)

Scenario	Comment
EMEP	Reported EMEP emissions
NVC, NVC32	TNO GNFR C emissions (and EMEP for other sectors) as non-volatile, C=Central (typical) TNO emissions. The runs with 32 suffix use 0.3x0.2 deg. lon/lat resolution, otherwise 0.1x0.1,
NVH, NVH32	As NVC, but with TNO 'High' (H) emissions
SVC32	As NVC32, but semivolatile OA from RWC allowed to evaporate (uses 1-5D VBS), see Sect. 4.2.
SIVC32	As SVC32, but with added intermediate volatility compounds, see Sect. 4.2.

4.1 Non-volatile POA setup

In the standard EMEP model setup used for policy runs (e.g. Fagerli et al., 2020, 2021), POA from all sectors are treated as inert, and formation of both anthropogenic and biogenic secondary organic aerosols (SOA) from anthropogenic and biogenic VOC precursors are taken into account. This assumption of inert CPOA has been justified by a number of factors

1. All treatments of both primary and secondary organic aerosol have large uncertainties. For POA these uncertainties include the need to specify volatility distributions, enthalpies, and the amount of any associated IVOC (e.g. Robinson et al., 2007, Grieshop, 2009, Jathar et al., 2017, Murphy et al., 2017, Simpson et al., 2020.). For SOA there are problems with estimating the emissions of precursors, and the SOA formation mechanisms themselves (Hallquist et al., 2009, Bergström et al., 2012, Hodzic et al., 2016, Murphy et al., 2017)
2. The "scientific" treatment of CPOA would need some rather arbitrary choices concerning these volatility distributions, enthalpies, and IVOC, which would then imply that PM_{2.5} emissions reported by countries would be allowed to "evaporate". Adding IVOC (either as some fraction of POA or NMVOC emissions) might be justified scientifically, but in this case emissions are being added on top of the officially reported PM and/or NMVOC emissions. The amount of IVOC to be added is very unclear with current scientific understanding, but these components can result in substantial changes in modelled PM_{2.5} (e.g. Murphy et al., 2017). Such decisions on CPOA and IVOC may be sensitive politically, and require much discussion within the EMEP system.
3. Earlier studies, e.g. from Robinson et al., 2007 and Simpson et al., 2012, had indeed suggested that the simple assumption of inert POA results in modelled PM_{2.5} which is quite similar to that obtained with more complex POA handling, though these earlier studies also included some additional intermediate volatility compounds along with POA emission.

Given all these uncertainties and issues, the "non-volatile" (NV) treatment of CPOA represents the simplest possible approach for CPOA used in this study. We explore the central and high TNO emission scenarios (NVC, NVH) as well as lower resolution (NVC32) simulations.

4.2 VBS setup

Equation [3] provides the underpinnings of the treatment of organic aerosol in many chemical transport models, including the EMEP model. Application is complicated by many factors, not least that many 1000s of compounds can be involved in OA emissions and formation, and each compound will have its own values of C_i^* (and of enthalpy). In order to make this complexity tractable, the volatility basis set (VBS) framework, developed by Donahue et al. (2006), Robinson et al. (2007) and others, lumps organics into logarithmically spaced bins of C_i^* values (defined at 298 K). For example, a bin with C_i^* of 10 $\mu\text{g}/\text{m}^3$ would have $\log_{10}(C_i^*)$ of 1.0, and include all compounds whose individual C_i^* values lay between $\log_{10}(C_i^*)$ 0.5 – 1.5. This range

corresponds to C_i^* of 3.2 – 32 $\mu\text{g}/\text{m}^3$. From Eqn [3], this class of compounds would partition 50:50% between the gas and particle phase if ambient C_{om} levels were around 10 $\mu\text{g}/\text{m}^3$, but almost all would evaporate if ambient C_{om} dropped to around 1 $\mu\text{g}/\text{m}^3$.

In many studies the different C_i^* bins are grouped into volatility classes such as "extremely low"-, "low"-, "semi"-, and "intermediate"- volatility compounds (ELVOC, LVOC, SVOC, IVOC, e.g. Robinson et al., 2007, Murphy et al., 2014), though exact definitions vary slightly between different studies. The term SVOC is also often used loosely as a term for all compounds which may experience partitioning in normal EF measurements (i.e. CPOA), and IVOC is used for compounds which can be regarded as 100% gaseous in such conditions. For clarity, we will use these looser definitions in this report.

For RWC, as well as the model runs with the inert POA assumption, we also test more advanced VBS-based schemes which are based upon experiments and analysis conducted at the Paul-Scherrer Institute (PSI) in a series of studies (Bruns et al., 2016, Ciarelli et al., 2017a). Bruns et al. (2016) determined that SOA precursors traditionally included in models account for only ~3–27% of the observed SOA from RWC emissions, and could explain ~84–116% of the SOA by inclusion of non-traditional precursors. Although hundreds of organic gases are emitted during wood combustion, SOA was estimated to be dominated by the ageing products of only 22 compounds. In some cases, oxidation products of phenol, naphthalene and benzene alone comprised up to ~80% of the observed SOA in these experiments.

Ciarelli et al (2017a) constructed and constrained a "1.5" dimensional VBS set (cf. Koo et al., 2014) to explain these observations, which was subsequently used in other PSI studies (e.g. Ciarelli et al., 2017b, Jiang et al., 2019). The measured POA was firstly partitioned across the volatility bins of the VBS system using the same recommended mass fractions in different saturation concentration (C_i^* , see Sect. 2) as used in Koo et al. (2014), with allocation of 20%, 10%, 10%, 20% and 40% to the C_i^* bins of 1, 10, 100 and 1000 $\mu\text{g}/\text{m}^3$ for biomass burning. Additionally, Ciarelli estimated an emission of "non-traditional VOC" (NTVOC), which they assigned as one IVOC compound with C_i^* of 10^6 $\mu\text{g}/\text{m}^3$. Given this setup, Ciarelli determined the yield parameters for the SVOC formed from POA, and that the NTVOC amounted to 4.75 times the mass emission of the POA compounds. Figure 11 illustrates this setup, with the POA compounds being split into the red bars from $\log_{10}(C_i^*)$ of -1 to 3 (though in the modelling the -1 and 0 bins were merged), and the NTVOC emissions placed at $\log_{10}(C_i^*)$ of 6.

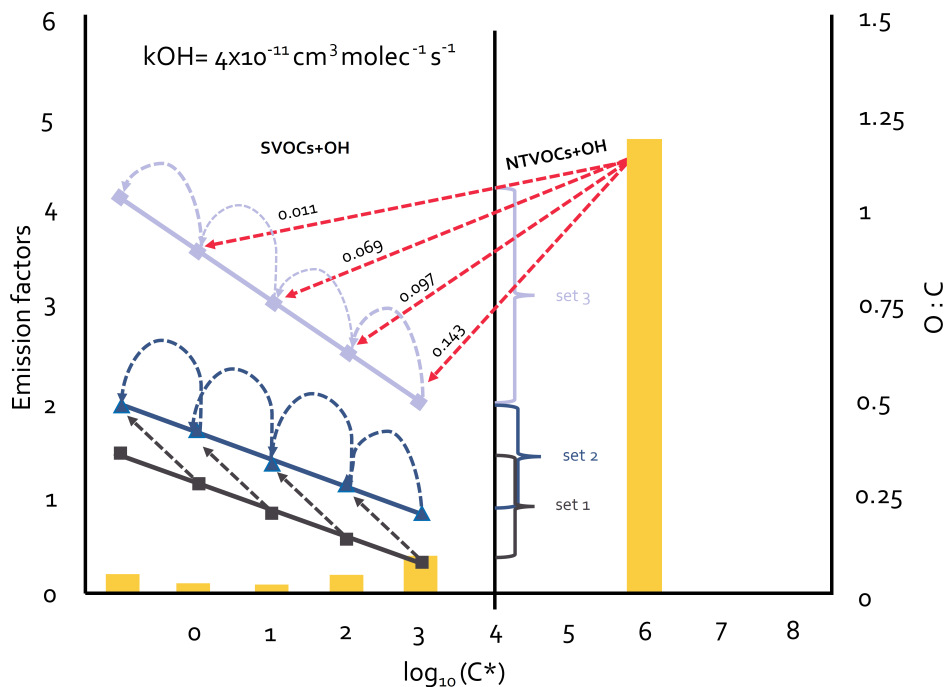


Figure 11. The "PSI" oxidation scheme: an average mixture of NTVOCs compounds are allowed to react with the hydroxyl radical following a naphthalene kernel mass distribution. Secondary products in the SOA set (set 3) are allowed to further react with a reaction rate of $k_{OH} = 4.0 \times 10^{-11} \text{ cm}^3/\text{molec}/\text{s}$. Oxidation products from semi-volatile vapours from the POA set (set 1) are allowed for further aging in set 2. The numbers on the red arrows indicate the NTVOCs yields for each bin for the best-fitting solution (ppm/ppm). From Ciarelli et al 2017a.

In the EMEP modelling done for this study, we assumed that the solid-particle (FPOA) data from TNO correspond to the lowest volatility C^* bins of $1 \mu\text{g}/\text{m}^3$ and below, and distributed the remaining CPOA across the 10, 100 and $100 \mu\text{g}/\text{m}^3$ bins in the same proportion as with the Koo et al/PSI schemes.

In some runs (denoted SIV), the PSI scheme's NTVOC emissions are added to the model as IVOC, again following the PSI scheme. As discussed above, this "IVOC" compound is a surrogate for many different VOC compounds, ranging from C3 to C16. A potential difficulty is that some of these compounds (especially the lighter ones, e.g. with $\leq C12$) are certainly included in the national VOC reporting, and so there is the potential for double counting some SOA precursor gases. However, Bruns et al do not provide the quantitative information that would be needed to omit or modify these VOC emissions, and it is anyway likely that different countries use different methods and definitions of VOC emissions in their reported NMVOC from RWC. It is also not known how the different TNO scenarios would affect the VOC emissions which should be included in the models.

It is also important to note that all aspects of the POA and IVOC partitioning are very uncertain, with many ratios of e.g. SVOC/POA or IVOC/POA or IVOC/NMHC given in the literature (e.g. Shrivastava et al., 2008, Jathar et al., 2017, Murphy et al., 2017). Given all these uncertainties, we accept the risk of double-counting of IVOC for this study, and so can regard the results of the "SIV" model scenarios (see below) as an upper-bound on the OA forming potential of RWC emissions for the setup we are using.

4.3 Residential wood-combustion emissions

In the EMEP model the residential wood-combustion (RWC) emissions are introduced into sector 'C' of the so-called GNFR emissions databases. The spatial distribution is provided here by TNO as part of the Ref2_v2.1 emissions. The temporal distribution within each model grid-cell is determined using heating-degree-days (HDD), as described in Simpson et al. (2012). Briefly, the emissions are assumed to be proportional to the difference between ambient temperature T and a base temperature T_{base} , which is 18°C (days with T above T_{base} have zero emissions). These variations are pre-calculated and normalised to ensure that the resulting annual emissions match the national reported emissions (or in this study, the TNO Ref2_v2.1 emissions).

One possible source of uncertainty is whether the 18°C T_{base} , which is thought to be appropriate for energy needs in general, is appropriate for wood-combustion, or whether a lower T_{base} would more reflect RWC usage. Denby et al (2011) used $T_{base}=11^{\circ}\text{C}$, which was found to work well in Norway. Grythe et al. (2019) explored T_{base} of 5, 10, and 15°C (also for Norway), and found that HDD5 produced the best model-measurement fit for benzo(a)pyrene and BC.

4.4 Levoglucosan

Levoglucosan (LG) is a major fraction of biomass burning emissions, that has frequently been used as a tracer of RWC (Simoneit, 1999, Gelencser et al., 2007, Szidat et al., 2004, 2009, Yttri et al., 2009, 2015, Zotter et al., 2014, Kaskaoutis et al., 2022). Although levoglucosan is likely to degrade in the atmosphere (e.g. Hoffmann et al., 2010), and is thus not truly inert, it is often found to correlate well with other markers of wood combustion, such as potassium or modern carbon (e.g. Zotter et al., 2014), and it is the best chemical marker we have for RWC in the EMEP measurements to be discussed in Sect. 5.

The OC/LG ratio in POA is however very variable, depending on the type of wood burned and combustion conditions (Hedberg et al., 2006, Kaskaoutis et al., 2022). A large number of studies concerning the emission ratio is available, and their suitability with respect to European conditions has been discussed by Gelencsér et al. 2007, Puxbaum et al., 2007, Simpson et al., 2007 and Yttri et al. 2011. Yttri et al. 2011 derived central values of LG/OC of 11.7% for $\text{PM}_{2.5}$ and 8.5% for PM_{10} for Norwegian conditions. Yttri et al. 2021 used LG/OC of 9.0% for $\text{PM}_{2.5}$ and 7.9% in PM_{10} . Zotter et al (2014) used ^{14}C measurements to derive values of non-fossil OC to LG of 12.6 ± 3.1 , hence LG/OC of 6.4–10.5%. Most estimates of LG/OC cover the range 6–15%, though higher values have been found (e.g. 22% in Greece by Kaskaoutis et al., 2022).

For this work, we assign an LG/OC emission rate of 10% of the POA carbon emissions, recognising that this ratio is very approximate and could perhaps be assigned an uncertainty of a factor of 2 (from 5% to 20%). We further assume that levoglucosan is an inert pollutant. This is also a common assumption which may be

inaccurate for long travel times, but is probably adequate for our purposes.

The longest database for levoglucosan measurements is from Birkenes in southern Norway (Yttri et al., 2021), which has data from 2008 onwards. The LG data at this site are impacted by sources over a large area of northern and central Europe (Yttri et al., 2021), and so the site is suitable to infer trends in RWC emissions over this large area. The most spatially extensive set of levoglucosan in Europe is that of the EMEP Intensive Measurement Period Winter 2017/2018 (<https://actris.nilu.no/Content/?pageid=66db6256b3f84b5b990efa04af7fe678>). Both sets of data are discussed in Sect. 5 and used in the model evaluations of Sect. 6.

5. Measurements

In this section we briefly summarise the measurements against which the new emissions and model results are compared. In general, these consist of the EMEP EC/OC data from the EMEP monitoring network, which provide data with long time-series which can be used to evaluate trends, and have a reasonable spatial coverage.

Observations of total carbon (TC), elemental carbon (EC), and organic carbon (OC) have been reported from a few sites to EMEP since 2000, but the earlier observations are hampered by the lack of comparable methodology. Since 2010 harmonisation of methodology using thermal-optical analysis according to the EUSAAR-2 temperature program (Cavalli et al., 2010) has been implemented at most sites. Excluding the mountain sites, there are 13 sites with sufficient data coverage which can be used for a regional scale trend analysis of EC/OC from 2010 to 2019. The number of sites with long term monitoring reporting EC/OC to EMEP and/or to ACTRIS has increased to 31 in 2019.

Levoglucosan is not part of the mandatory EMEP measurement programme (Level 1 or level 2) as defined in monitoring strategy (UNECE, 2019), but identified as voluntary level 3 observations to assess the contribution of different sources to organic aerosols. Levoglucosan is also included in the ACTRIS programme. However there are relatively few sites reporting levoglucosan data to EMEP and ACTRIS on a regular basis. For trend analysis, it is only data available from one site with sufficient coverage, Birkenes, (Yttri et al 2021).

We have also used data from the EMEP Intensive Measurement (EIMP, Platt et al., 2019), December 2017 - March 2018. EMEP/ACTRIS/COLOSSAL arranged a winter campaign on apportionment of equivalent black carbon (EBC) into fossil fuel and wood burning at sites with hourly multi wavelength measurement of the absorption coefficient, combined with off line 24-168h measurements of levoglucosan and EC/OC. 57 sites participated including 4 global sites, 26 regional background sites and 27 urban background sites. Of these, 49 sites measured levoglucosan and 52 OC/EC. In this work, we have excluded the urban and global sites to better compare with the EMEP model on a regional scale. Further, only those sites with both EC/OC and levoglucosan measurements have been used. With this screening, observations from 23 sites have been used (Figure 12).

The regular observations and most of the data from the intensive period are available from EBAS (<https://ebas.nilu.no>). All the observations from the EIMP are compiled by Platt et al (2022).

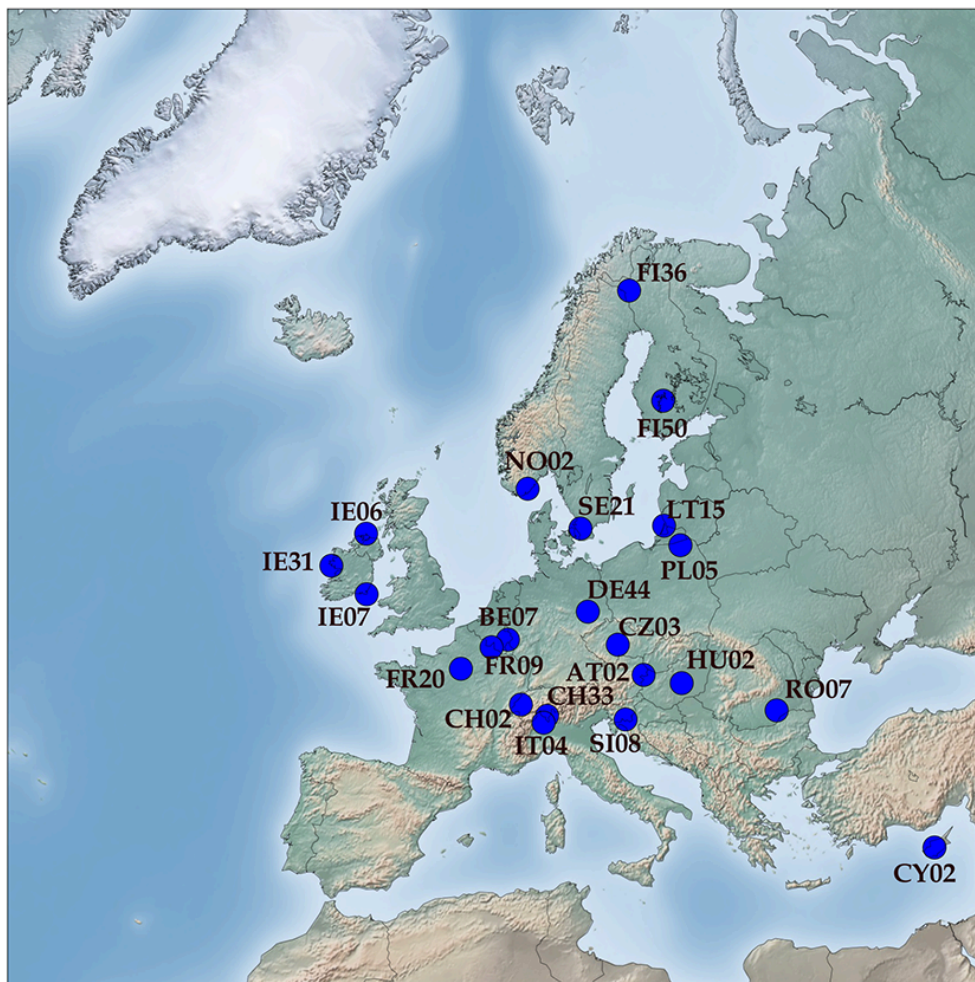


Figure 12. Overview of the sites used for EC, OC and levoglucosan measurements from the EMEP intensive measurement period winter 2017/2018. Remote (Zeppelin Observatory (NO42) and Sonnblick (AT34)) are not included.

6. Comparison of modelled versus observed concentrations and trends

6.1 The winter 2017/2018 campaign

Tables A1–A3 show the modelled versus observed OC, levoglucosan, and EC for the 3 months of the main EIMP campaign, and Figs. 13–15 presents scatter plots of these data for the different model scenarios. Considering OC first, although the individual site correlations seen in Table A1 are very variable, the overall agreement seen in Fig. 13 is very good in terms of correlation, with R-values ranging from 0.80 to 0.91. The slopes of the regression lines vary markedly though, from just 0.25 in the SVC32 case (where POA has been allowed to evaporate) to the extremely good value of 1.02 in the NVH case.

At first sight the very good performance in the NVH case might be an argument that the high emission factors are more realistic, but we can note that the high correlations seem to be driven by the highly polluted sites (with OC from ca. 6–10 $\mu\text{g}/\text{m}^3$) such as HU02, RO07 and IT04. The NVH runs strongly overestimate OC at several of the less polluted sites, such as NO02 or FI36 (cf. Table A1). Similar results in terms of overall scatter and individual sites are seen for levoglucosan, and EC.

It is also important to note that many discrepancies between modelled and observed concentrations may be due to other issues, such as meteorology and dispersion, so we should not try to ascribe all discrepancies to emissions. For example, even though the EMEP model captures NO_2 on average very well across Europe, the model overpredicts NO_2 at Birkenes (NO02) during these three months by a factor of 2.4, so the overprediction of OC, EC and levoglucosan here is likely at least partly due to dispersion issues rather than emissions. Other examples of modelled/observed NO_2 ratios are 0.88 for Ispra (IT04), 0.76 for Illmitz (AT02), 0.73 for Diable Gora (PL05) and 1.46 for K-Pusztá (HU02). Discrepancies are also expected to be higher in the situations where OC (or other pollutant) levels are elevated, since atmospheric conditions often include stable boundary layers and stagnant conditions which can be difficult to resolve with meteorological drivers and CTMs. There is also the possibility that especially RWC emissions increase during such periods, more than predicted by the model's heating-degree-day system (Sect. 4.2), since wood-burning may be used to supplement energy needs in extreme cold.

Comparing NVC with NVC32 in Figs. 12–14 and Tables A1–A3, we can note that the benefits of 0.1x0.1 deg resolution compared to 0.3x0.2 are seen to be large as far as bias is concerned, but that R values may increase or decrease for different sites.

As noted in Sect. 5, the EBC data from this campaign are still under analysis. Results presented in Platt et al. (2019) and the latest analysis suggest quite low biomass burning fractions ($\text{BBF} = \text{EBC}_{\text{bb}}/\text{EBC}_{\text{tot}}$) of less than 50% at many sites. The current model results would suggest much higher BBF values (here $\text{EC}_{\text{bb}}/\text{EC}_{\text{tot}}$), especially at sites in southern and Eastern Europe, such as Ispra (IT04, ca. 80% for NVC), K-Pusztá (HU02), Illmitz (AT02) with 60–80% BBF from the model. This

apparent discrepancy may reflect problems in the EC emissions from Ref2_v2.1, but further work is required to analyse these data. (In any case, the focus of this study is on OC rather than EC.)

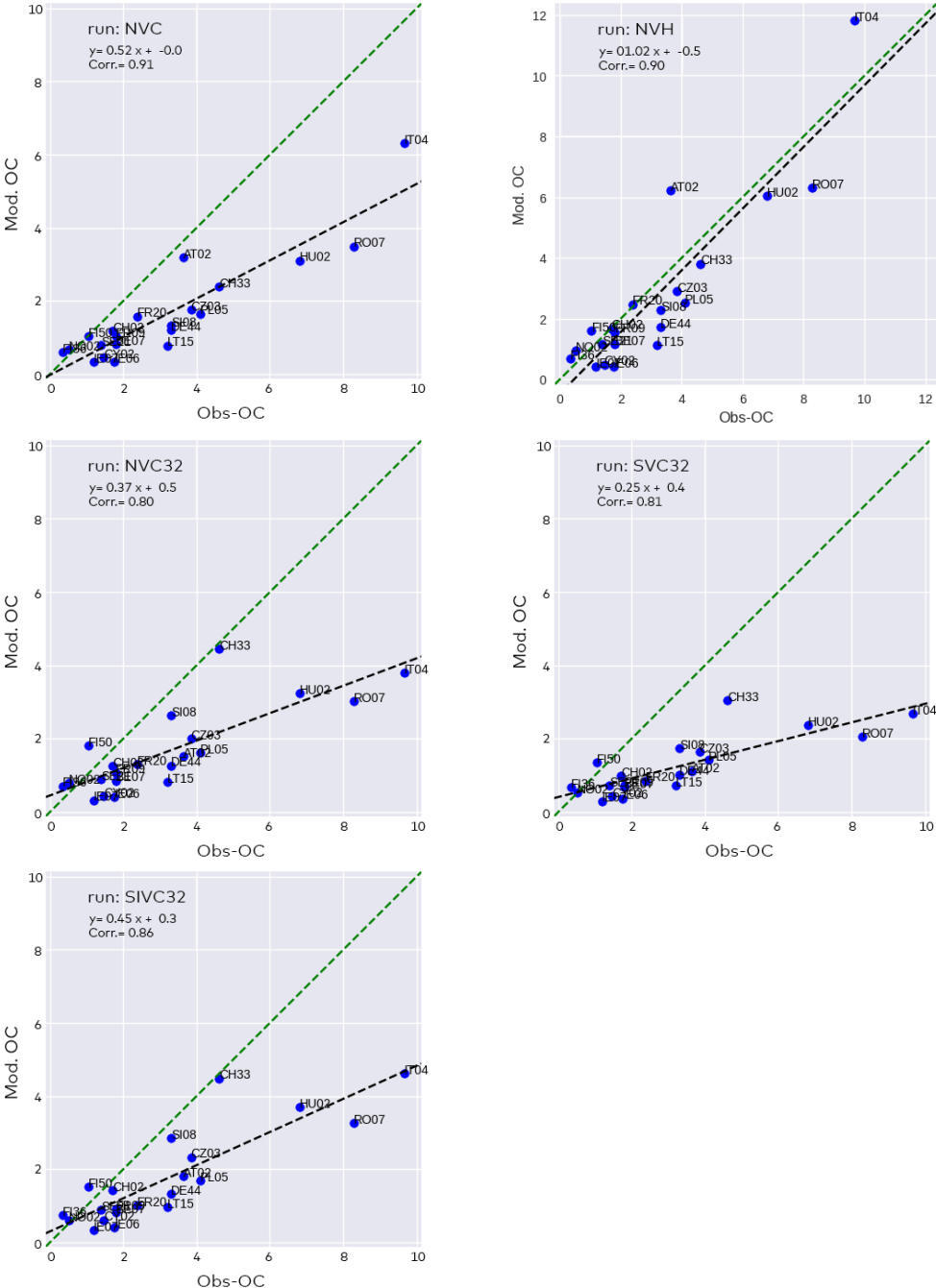


Figure 13. Modelled versus observed OC ($\mu\text{g}/\text{m}^3$) for the EIMP campaign, rural sites. Black dashed line is regression line. Green dashed line is 1:1 line.

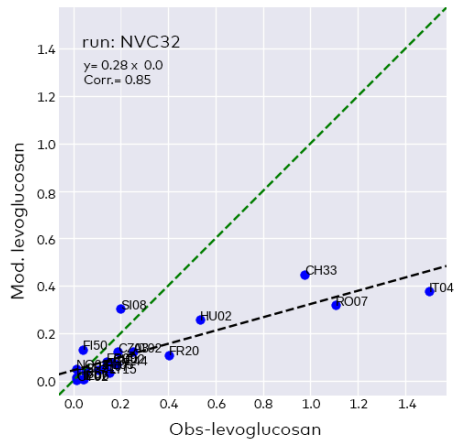
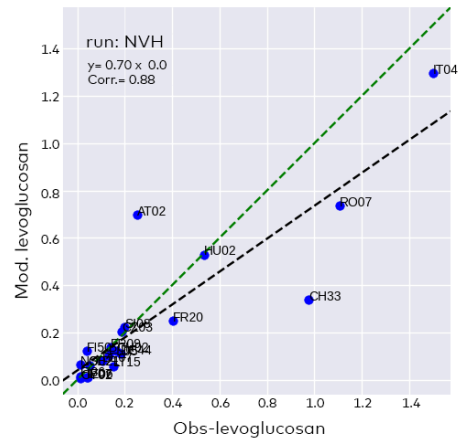
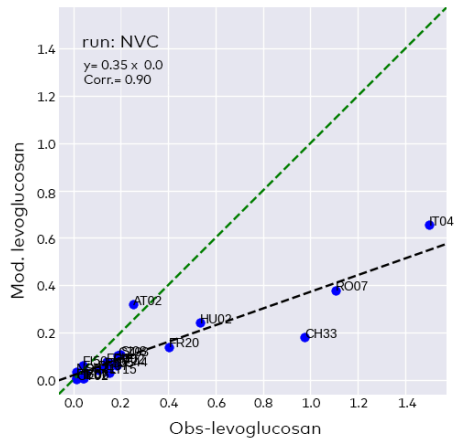


Figure 14. As Fig. 13, but for levoglucosan.

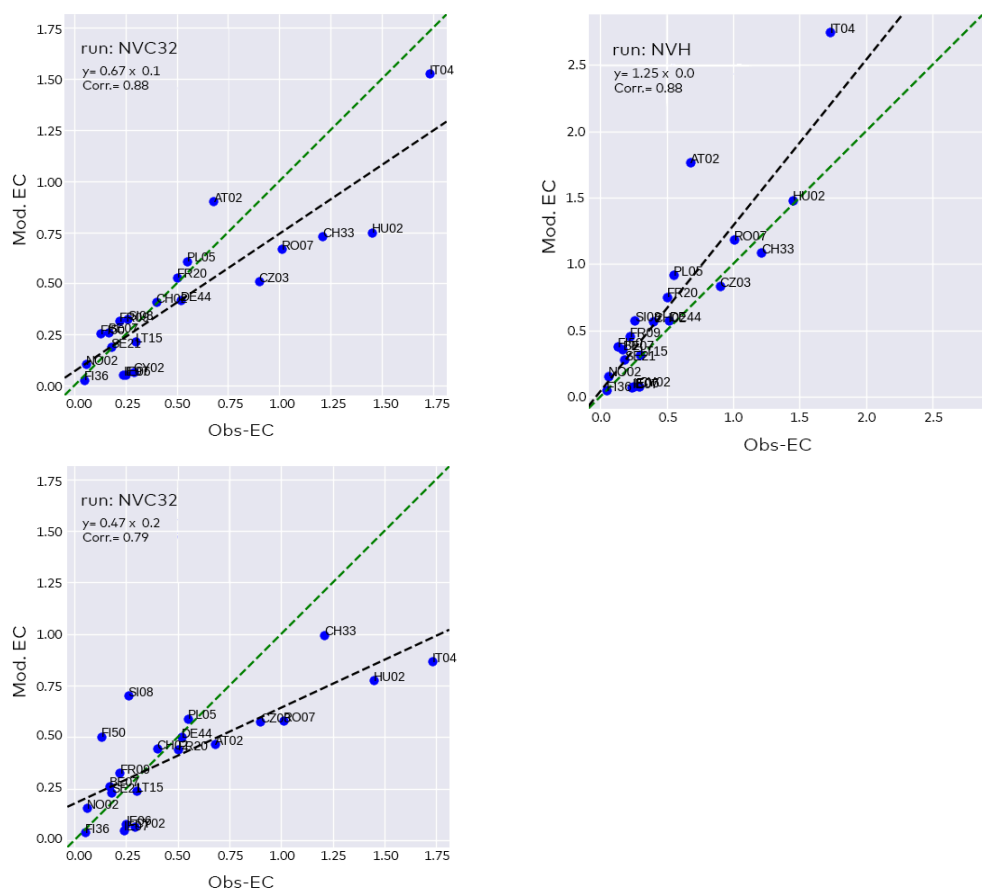


Figure 15. As Fig. 13, but for EC.

6.2 Modelled versus observed trends

In this section we present modelled versus observed trends over the period 2010–2019, and for the winter (December-January-February, DJF) months. The 2010–2019 period is chosen due to the expanded number of sites measuring OC and EC during this period. The DJF period is chosen to help isolate the impacts of RWC emissions. (During the spring months OC may be affected by primary biological aerosol, and in summer time secondary organic aerosol formation is an important source, e.g. Gelencser et al., 2007, Yttri et al., 2011, 2021.)

The trends were calculated using MET Norway’s pyAerocom software (<https://github.com/metno/pyaerocom>). Yearly trends were calculated only for stations where at least seven years of valid data was available. A valid year was defined as a year where all four seasons had a minimum of one month of observations. A month had to be made up of at least four days, which in turn had to have at least 18 hours, themselves consisting of 45 minutes or more. Stations which did not have the desired amount of valid years were excluded from the trend calculation. From here, the trend for each station was calculated using yearly data and a Theil–Sen estimator used for the linear regression. The p-value of the linear regression was calculated using Kendall’s Tau test.

To find the trend for larger regions, such as countries or the whole of Europe, the mean of the individual trends at sites in the region was calculated. The error of the

regional trends was found by taking the standard deviation of the set of individual trends. The regional p-values were calculated by taking the harmonic mean of the individual p-values.

This is one of two ways of finding the regional trends, the other one being to calculate the regional timeseries, and then find the trend, error and p-value of this timeseries. Here the former method was used, since this makes the regional trends less sensitive to having stations pulling the trend in one direction. The downside of this method is that the trend line doesn't necessarily correspond well to the average regional timeseries which are plotted.

As the simplest example, Fig. 16 shows the modelled and observed trends for levoglucosan (LG) for Birkenes in southern Norway. As discussed in Sect. 4.3 (and Yttri et al., 2021), changes in LG at this site should reflect regional changes in RWC emissions. The three model scenarios differ in resolution (NVC has 0.1x0.1-degree resolution, versus NVC32 with 0.3x0.2 lon/lat resolution), and in terms of typical versus high emission factors (NVC32 vs. NVH32). It is clear that all model results produce rather similar trends of ca. -6%/yr, and that this matches the observed trend of -7.54% trend rather well, which gives some confidence to the magnitude of trends in the Ref2_v2.1 RWC emissions in northern and central Europe. The different model setups do tend to overestimate LG at this site, but as noted in Sect. 4.3 the emission rate assigned to LG was only indicative, and a factor of two uncertainty is not unreasonable. In any case, a similar overestimate can be seen for NO₂ in the DJF periods, so factors other than emissions (e.g. difficulties with wintertime stable boundary layers) likely play a role.

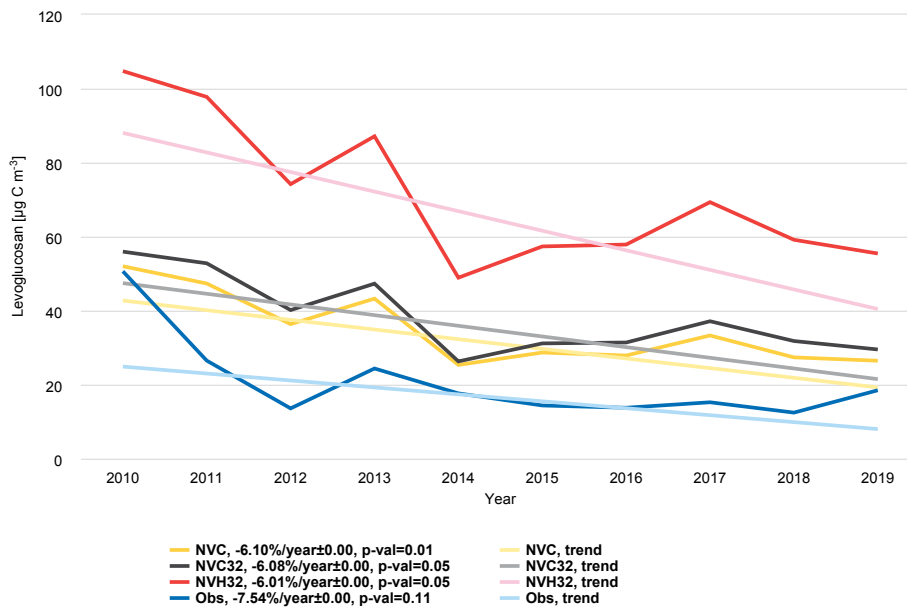


Figure 16. Modelled versus observed 2010–2019 trends in DJF levoglucosan at Birkenes (NO₂, Norway) over 2010–2019. Solid lines give average DJF concentrations, and straight lines give the trends calculated for different model setups. See text.

Fig. 17 illustrates a similar trend analysis, but for OC in PM_{2.5} sample at the Slovenian site Iskra (SI08). For this site the observations are higher than in most model setups for most years, and the observed trend is stronger (-4.9%/yr) than the modelled trends. The latter vary significantly though, from -2.07%/yr for NVC to -3.91 %/yr for SIVC32, suggesting that the assumptions concerning volatility and/or IVOC emissions can have a strong influence on the calculated trends, and on the agreement with observed trends.

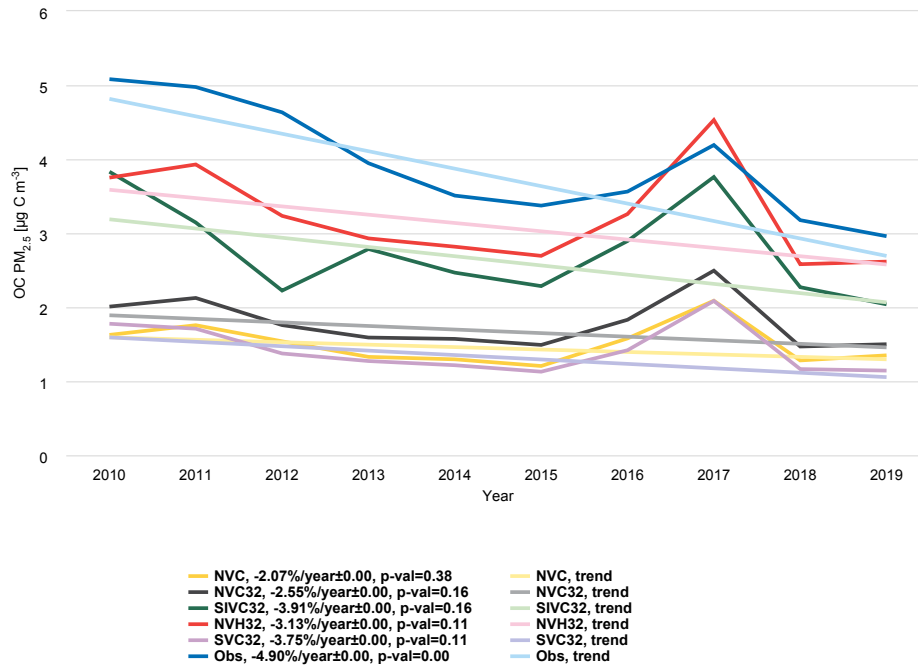


Figure 17. Modelled versus observed 2010-2019 trends in OC in PM_{2.5} samples DJF period for the site SI08 (Iskra) in Slovenia. Solid lines give average DJF concentrations, and straight lines give the trends calculated for different model setups. See text.

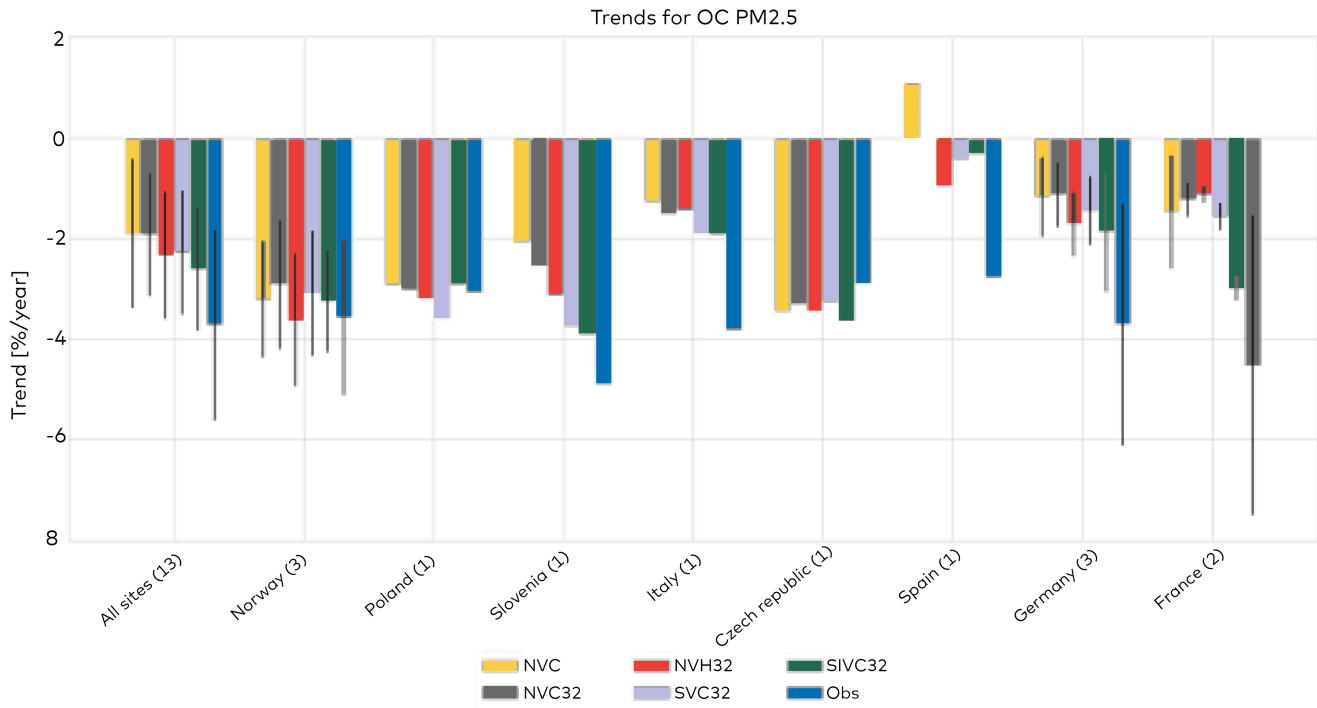


Figure 18. Comparison of calculated DJF trends over 2010–2019 with five model scenarios, compared to measurements. Numbers in brackets give the number of sites. Here, the trends give the average of the individual trends calculated for each site, and error bars indicate the standard deviation (σ) among sites where relevant.

It is difficult to consider trends at all sites together, since many sites did not start operations in 2010, and there are data-gaps also. However, as explained above, we can calculate the trends for each site (requiring a minimum of 7 years of data), and plot the averages of these trends to get a better understanding of the overall reductions in OC and PM_{2.5} over the measurement network.

Figure 18 shows these calculated trends, both for all 13 sites, and also for individual countries. The “All sites” data show that the NVH, SVC32 and SIV32 give improved trend estimates compared to the observed trends, although still somewhat low. The Slovenian site shows a clearer progression, but for other sites (Norway, Czech R.) the different model setups give more mixed results. In general the SIVC32 runs come closest to observed trends, and several locations (Norway, Poland, Slovenia, Czech R.) show rather good agreement with the magnitude of the observed trends. At the Spanish site (Montseny) the model results usually overpredict the absolute values of the OC concentrations (not shown), and give very different trends to the observed. The high elevation (704m) of this site may complicate this comparison.

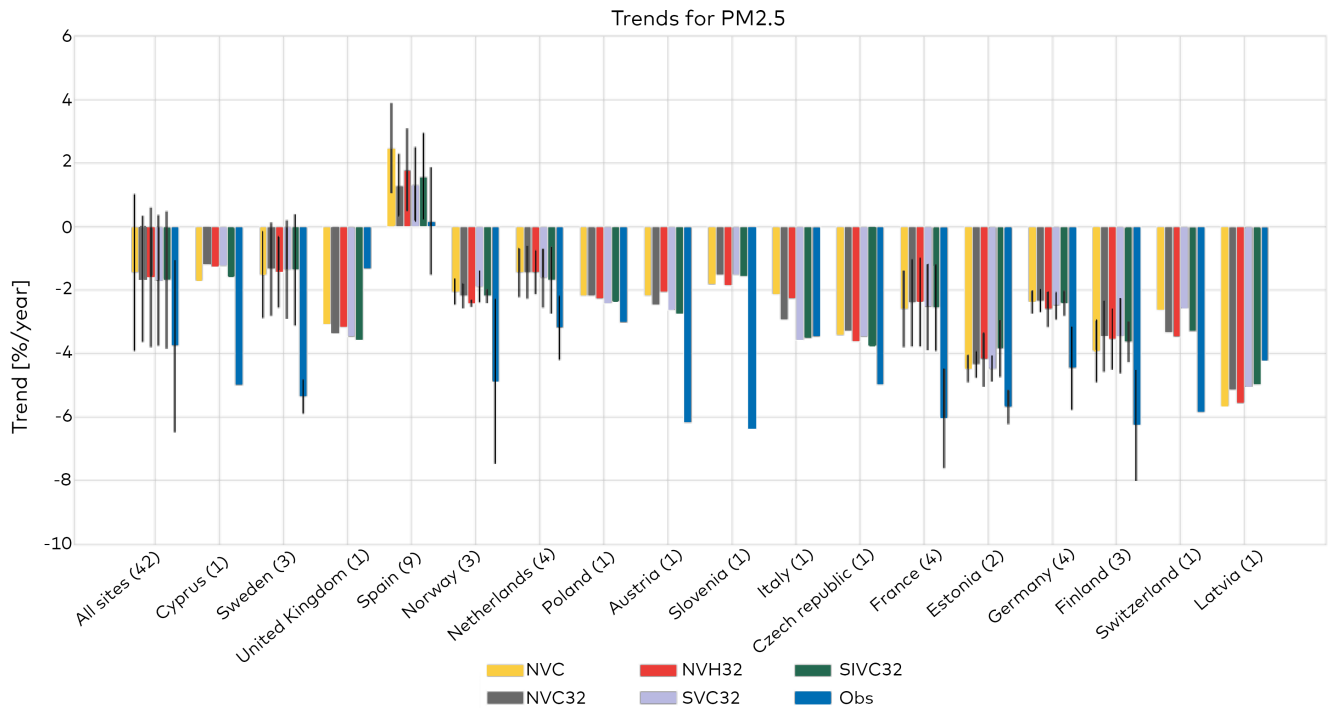


Figure 19. As Fig. 18, but for $PM_{2.5}$ trends.

Figure 19 shows the 2010–2019 trends from different model scenarios and observations for $PM_{2.5}$ in winter time (DJF). For $PM_{2.5}$, the trend based on annual averages (not shown) are slightly underestimated in all model scenarios (-2.1 to -2.3%/yr compared to -3.1%/yr in observations). For winter time (DJF), the underestimation of the trend is much larger (-1.3 to -1.7%/yr compared to -3.6%/yr in observations). In order to investigate how much of this underestimation of the winter trend in $PM_{2.5}$ that is caused by the underestimation of $OC_{2.5}$ winter trends (and difference in absolute levels), we made a new series of trend calculations for $PM_{2.5}$ ($PM_{2.5}$ -Corrected) where the modelled concentrations for $PM_{2.5}$ were corrected for the bias in the OC calculations. Out of the 13 sites that had $OC_{2.5}$ measurements, 12 of them had measurements of $PM_{2.5}$ (all sites except Observatoire Perenne de l'Environnement). For those 12 sites, we calculated (for DJF) the corrected $PM_{2.5}$;

$$PM_{2.5}\text{-Corrected} = PM_{2.5} + OM_{\text{bias}}, \text{ where } OM_{\text{bias}} = (OC_{\text{obs}} - OC_{\text{mod}}) * OM/OC$$

OM is organic matter, and OM/OC is the ratio of the OM to OC mass in $\mu\text{g}/\text{m}^3$. OC_{obs} and OC_{mod} are the observed and modelled OC concentrations (in $PM_{2.5}$) for DJF in $\mu\text{g}/\text{m}^3$. The OM/OC ratio was set to 1.8, a value which is approximate, but consistent with both the model results for this DJF period and within the ranges 1.6–2.1 suggested by Turpin and Lim (2001) for urban and non-urban aerosol. (OM is available directly from the EMEP model, but not yet implemented in the pyAeroval system we use for these trends.) Note that the frequency of the OC and PM measurements are not always the same, e.g. several of the OC sites have measurements only every third day, whilst $PM_{2.5}$ measurements are mostly daily. However, by doing this on a seasonal basis (DJF), this should give a reasonable estimate of the contribution of OC to $PM_{2.5}$.

We made this correction for all the different scenarios, but the resulting corrected

PM_{2.5} concentrations are very similar for those that have the same resolution (as these model runs are mainly different in OC). The resolution of the model runs (0.1x0.1 vs 0.3x0.2 degrees) influences the results somewhat, as that is also affecting the other chemical components of PM_{2.5}. In the following, we have chosen only to focus on the NVC results (with the finer resolution), although the conclusions are the same using any of the other scenarios.

Figure 20 shows an example of the effect of the correction at the Ispra site. For Ispra, the correction is largest early in the period (2011–2013), bringing the PM_{2.5} level into close agreement with observed levels. The corrected trend (-3.88%/yr) is also in much better correspondence with the observed trend (-3.47%/yr) than in the original model run (-2.14%/yr). Figure 21 shows PM_{2.5} trends (corrected and original) for all the sites that have both PM_{2.5} and OC_{2.5} measurements. Overall the trends (9 out of 12 sites) calculated from the NVC-Corrected agree better with observations than the original NVC model run (On average: observations -4.7%/yr, NVC -1.9%/yr, NVC-Corrected -3.7%/yr). Furthermore, 10 out of 12 sites have a significantly improved normalised mean bias, with the average bias improving from around -17% to 2% for DJF 2010-2019, see Fig. 22.

A comparison of the PM_{2.5} DJF trends using only the 12 sites which had OC_{2.5} measurements and using all available PM_{2.5} measurements (42 sites) shows that they are relatively similar (observations: -4.7 and -3.8%/yr and model -1.9 and -1.5%/yr for 12 sites and all 42 sites, respectively), and we conclude that these 12 sites roughly represent the European trend for PM_{2.5}. Our results therefore suggest that the underestimation of the downward trend in modelled OC (and low wintertime levels) can explain a large part of the underestimation of the downward trend in PM_{2.5} in Europe for 2010–2019.

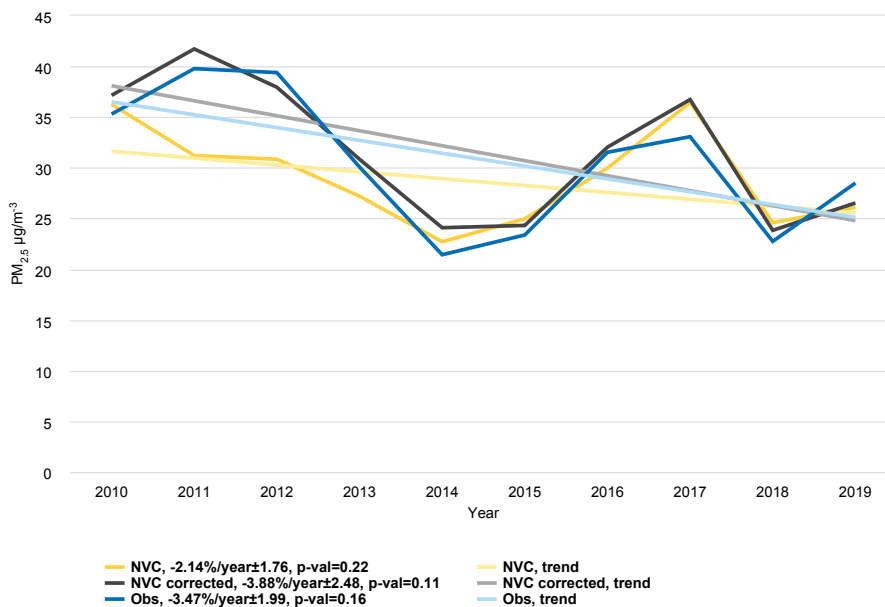


Figure 20. 2010–2019 trend for PM_{2.5} (DJF) at Ispra, for observations, NVC and NVC-Corrected.

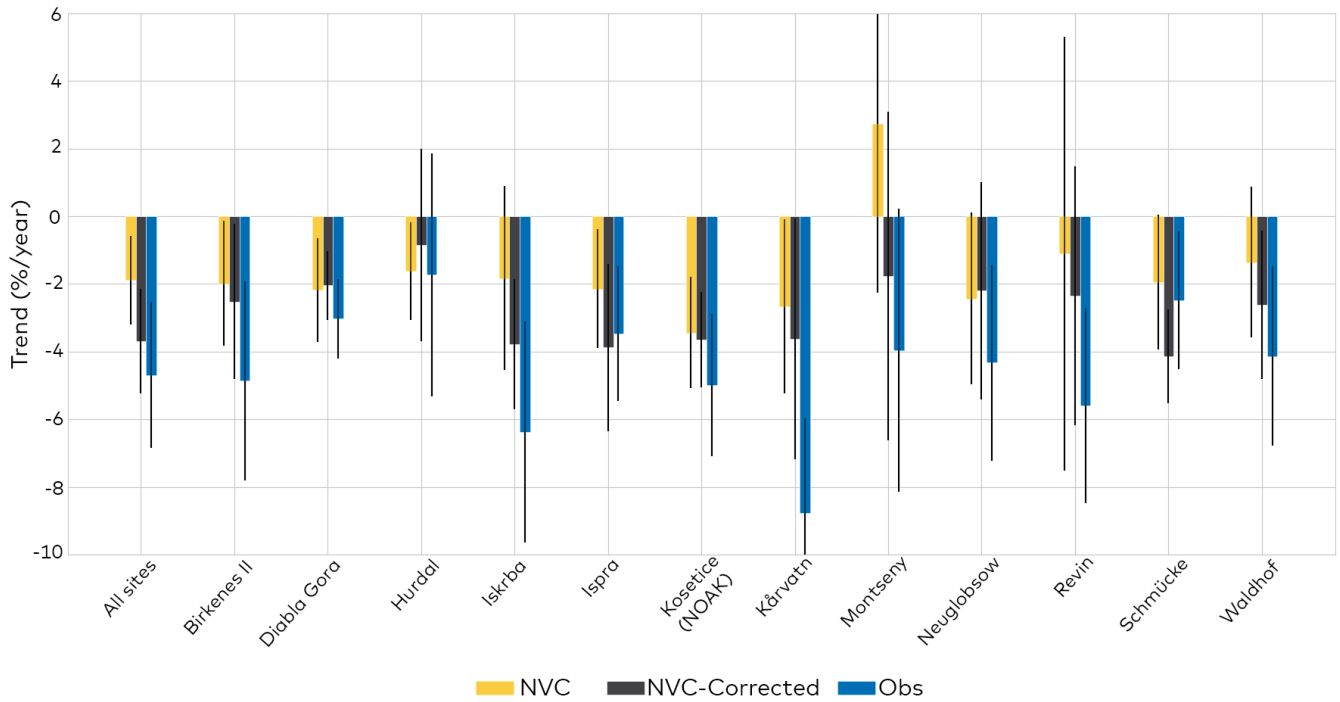


Figure 21. 2010–2019 trends for $PM_{2.5}$ (DJF) at all sites that have both $PM_{2.5}$ and $OC_{2.5}$ measurements, for observations, NVC and NVC-Corrected. For single stations, uncertainty bars represent the standard deviation (σ) of the mean of the trends.

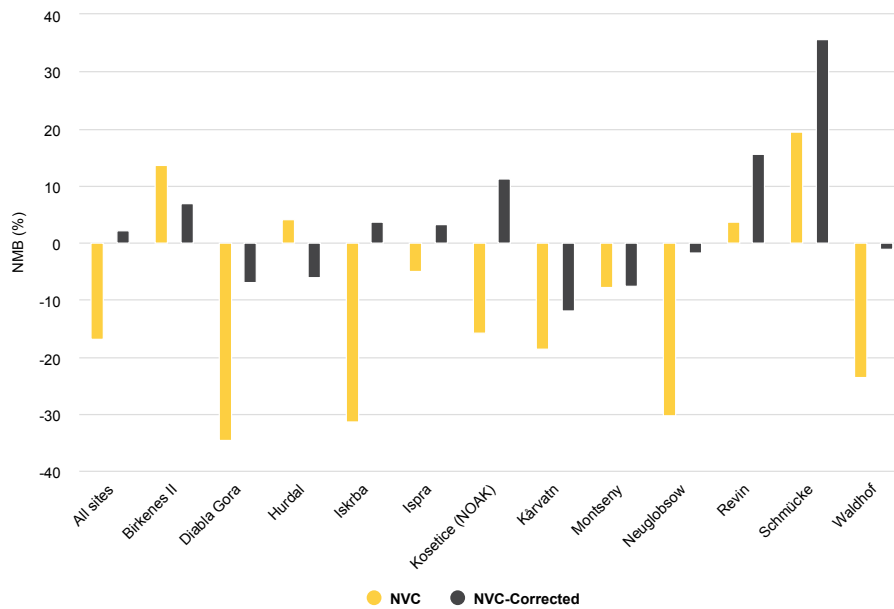


Figure 22. Normalised mean bias (2010–2019) for $PM_{2.5}$ (DJF) at all sites that have both $PM_{2.5}$ and $OC_{2.5}$ measurements, for NVC and NVC-Corrected.

7. Policy implications

The inclusion of condensables has a number of effects which can affect the scientific background to air pollution control policies:

1. Impacts the emission estimates submitted to the EMEP system
2. Impacts the modelled $PM_{2.5}$ and hence health-related impact studies
3. Impacts trend analysis, since the relative change in POA might be different to that of other primary (and secondary) PM emissions.
4. Impacts the relative contribution of different countries, including some improvement in the fairness of source-receptor matrices when the emission estimates become more consistent.

The impact of condensables and revised emission and model scenarios on OC, EC and $PM_{2.5}$ at various observation sites have been illustrated in Sect. 6, and on trends in Sect. 7, with a focus on the winter (DJF) period. Here we illustrate the larger scale changes in $PM_{2.5}$ (Sect 7.1), and some impacts on source-receptor matrices (Sect 7.2), both on an annual basis.

7.1 Impacts on $PM_{2.5}$

Figure 23 shows the difference in $OM_{2.5}$ and $PM_{2.5}$ between the NVC32 run and the default EMEP run (also $0.3 \times 0.2^\circ$) for 2016. The NVC32 case leads to increased $OM_{2.5}$ everywhere, and by over $2.5 \mu\text{g}/\text{m}^3$ in $OM_{2.5}$ (organic component of $PM_{2.5}$) and $PM_{2.5}$ in some areas (e.g. Poland). (Some small negative values for PM in some south eastern areas may reflect changes in PPM components other than POA, or different spatial distributions between EMEP and Ref2_v2.1 emissions). Figure 24 illustrates the geographical impact of the different Ref2_v2.1 scenarios compared to the NVC32 case. As expected from the site comparisons discussed in Sect. 6, the NVH32 scenario leads to substantial increases in $OM_{2.5}$ and $PM_{2.5}$ across Europe, but especially in the south-eastern regions. SVC32 gives lower concentrations, but SIVC32 again leads to increased $OM_{2.5}$ and $PM_{2.5}$ compared to NVC32 and hence EMEP across much of Europe.

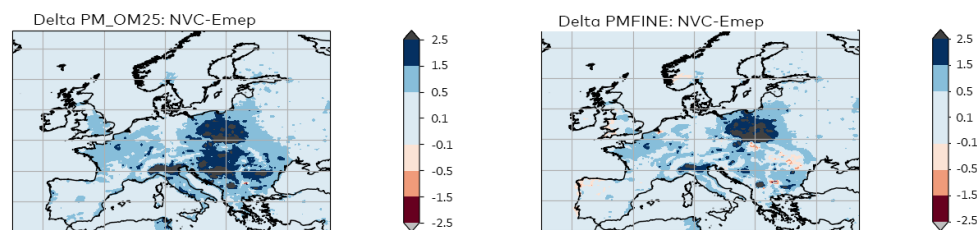


Figure 23. Deltas ($\mu\text{g m}^{-3}$) of $OM_{2.5}$ (left) and $PM_{2.5}$ (right) from Ref2 v2.1 scenarios compared to EMEP.

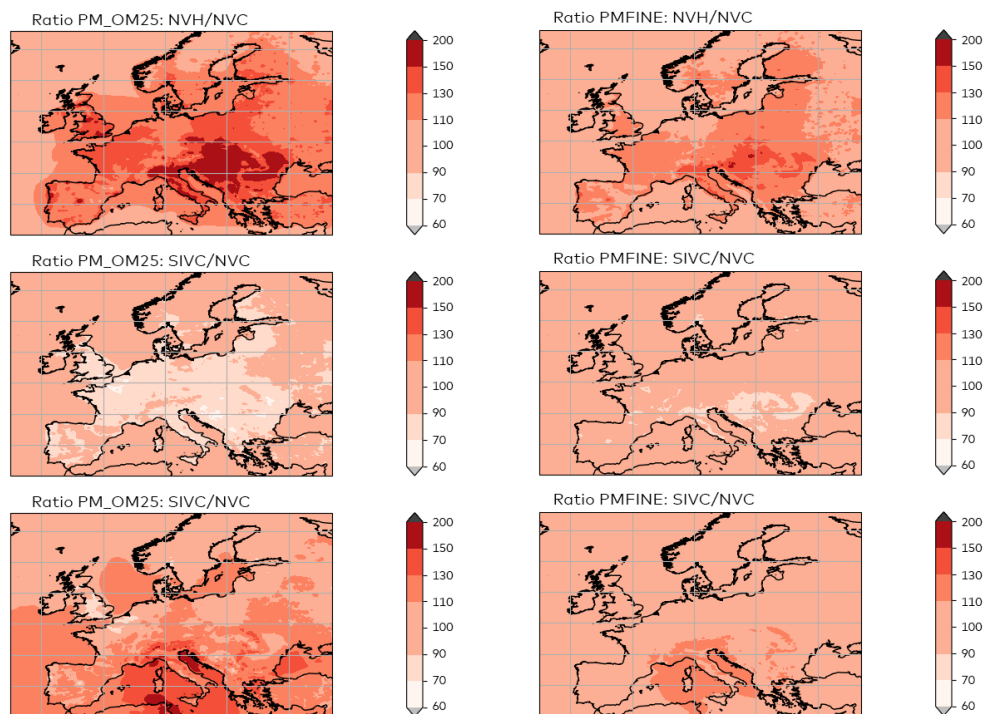


Figure 24. Ratios (%) of $OM_{2.5}$ (left) and $PM_{2.5}$ (right) from Ref2 v2.1 scenarios compared to NVC.

7.2 Source-receptor calculations

The EMEP model has been used in a series of moderate resolution (0.2° lat \times 0.3° lon) tests to evaluate source-receptor relationships. These tests have been conducted with five base cases: EMEP, NVC32, NVH32, SV32, SIV32. For each case we have reduced $PM_{2.5}$ emissions from Austria (AT), Germany (DE) and Italy (IT) by 15% in separate runs. The results are shown in Tables 5–7. The first numeric column of these Tables shows the average concentrations of fine PM over various example countries. The remaining columns give the changes in concentrations (ΔPM) caused by changes in $PM_{2.5}$ emissions from either AT, DE or IT.

In Table 5 the AT row shows that Austria's contribution to itself is substantially higher (by factors of 1.4–3.5) in all the Ref2_v2.1 cases than in the standard EMEP case; this reflects the omission of CPOA in the Austrian EMEP emissions, so that all Ref2_v2.1 cases have substantially higher national emissions (cf. Figs. 7, 9). The impact of AT on other countries is similarly increased with all Ref2_v2.1 scenarios. The NVH scenario has the biggest impact on the self-contribution (AT to AT), but the contributions of AT to other countries are often greatest with the SIVC32 scenarios. This difference reflects that the semi- and intermediate- volatility compounds of SIV scenarios require time for oxidation processes to convert the gas-phase compounds to secondary organic aerosols. Thus, the contributions of SVOC and IVOC will increase with transport distance.

The corresponding results for Germany are given in Table 6. Here the contributions of DE to itself and other countries differ, but less dramatically than in the Austrian

case. The NVH scenario again has the biggest impact on the self-contribution (DE to DE), and again the contributions to other countries are often greatest with the SIVC32 scenarios. Finally, the Italian results (Table 7) show similar features to those of Germany. The NVH scenario gives the biggest self-contribution, and the SIVC scenario has more impact on other countries.

In general, it is clear that the assumptions concerning volatility and inclusion of IVOC emissions have significant impacts on the source-receptor matrices. The simplest assumption of the NVC scenarios, namely inert CPOA, provides results which generally lie within the range of the SVC to SIVC scenarios, and the NVH scenarios give higher contributions. The NVC changes are generally within the ranges found for the SVC-SIVC scenarios. Given the many uncertainties associated with the emissions and the modelling of POA and SOA, these results indicate that the inert (NV) assumptions provide a reasonable first approach for handling POA emissions, which can hopefully be improved once our understanding of the sources and processing of POA improves.

Table 5. Source-receptor relationships derived from different base-cases, for 15% reductions in PM_{2.5} from Austria. Year: 2016. All runs here use 0.3×0.2 lon/lat resolution. The yellow row indicates the impact of emitter Austria on itself.

Receiver	Conc. PM _{2.5} μg/m ³	ΔPM / Δ Emis(AT)				
		EMEP	NVC	NVH	SVC	SIVC
AT	6,51	0,094	0,185	0,325	0,136	0,172
CH	5,65	0,003	0,007	0,012	0,006	0,011
DE	8,87	0,005	0,01	0,017	0,008	0,014
IT	10,14	0,002	0,003	0,005	0,003	0,009
RO	9,11	0,001	0,002	0,003	0,002	0,005
SI	9,82	0,019	0,038	0,065	0,032	0,054

Table 6. As Table 5, but for Germany

Receiver	Conc. PM _{2,5} μg/m ³	ΔPM / Δ Emis(AT)				
		EMEP	NVC	NVH	SVC	SIVC
AT	6,08	0,016	0,017	0,022	0,016	0,024
CH	5,64	0,019	0,02	0,027	0,019	0,025
DE	8,86	0,146	0,179	0,239	0,151	0,165
FR	6,22	0,009	0,011	0,014	0,01	0,014
IT	10,17	0,001	0,001	0,002	0,002	0,004
NL	11,74	0,051	0,064	0,082	0,057	0,064
PL	8,74	0,011	0,014	0,018	0,013	0,018
SI	9,78	0,004	0,005	0,006	0,005	0,01

Table 7. As Table 5, but for Italy

Receiver	Conc. PM _{2,5} μg/m ³	ΔPM / Δ Emis(AT)				
		EMEP	NVC	NVH	SVC	SIVC
AT	6,08	0,009	0,011	0,018	0,01	0,039
CH	5,64	0,017	0,021	0,036	0,018	0,056
DE	8,86	0,001	0,002	0,003	0,002	0,008
FR	6,22	0,005	0,006	0,01	0,006	0,024
IT	10,17	0,376	0,46	0,798	0,344	0,547
MK	8,95	0,002	0,003	0,005	0,003	0,015
SI	9,78	0,038	0,045	0,073	0,043	0,118

8. Conclusions

Condensable primary organic aerosol emissions are a class of organic compounds that are vapour phase at stack conditions, but which undergo both condensation and evaporation processes as the stack air is cooled and diluted upon discharge into ambient air. Emission factors measured in or close to the high-temperature high-concentration exhaust stack or pipe may misrepresent, and even miss, the amount of PM or gas that actually enters the atmosphere, depending on the filters, dilution and sampling conditions of the emission measurement. In the current emission reporting to EMEP/CLRTAP there is no clear definition of whether condensable organics are included or not, and, if included, to what extent.

A number of earlier studies (e.g. Denier van der Gon, 2015) have shown that these discrepancies have important implications for the consistency of emissions, and as a consequence for air quality modelling in Europe. At a workshop organised by EMEP/ MSC-W in 2020 (Simpson et al., 2020) it was agreed that condensables should be included in future emission inventories and modelling, with residential wood combustion (RWC) emissions as a priority source, although it was recognised that it is also important to take stock of other sources (e.g. road transport) that might prove to be important.

The workshop agreed that the TNO Ref2 emissions provide a good no-regret step towards a harmonised emission methodology, but that these top-down estimates should be increasingly replaced by national estimates once procedures for quantifying condensables in a more harmonised way are agreed on and implemented. During 2020–2022 these TNO Ref2 emissions have been used and updated, and several countries have also included condensables in the national reporting.

A major problem with the inclusion of condensables is that the emission factors (EFs) used depend heavily on measurement conditions, and there are no fixed guidelines for how to choose the appropriate EFs. Assessment of currently reported emission inventories show that there is a wide variation in implied emission factors for biomass, which cannot be explained by the inclusion of condensables and the variation in technology and abatement levels alone.

There is thus a strong need for consistent sets of RWC emissions, which can be used for both the modelling of air quality, and as a reference dataset against which national estimates can be compared. There have also been some major changes in reported RWC emissions over the last decade, and thus there is also a need for a consistent time-series of such emissions if we are to model changes since 2005.

In this study, new residential combustion emission estimates have been developed for the years 2005–2019 (called TNO Ref2_v2.1) in a consistent manner, with improved estimation of fuel consumption (in particular wood) as well as an updated split of fuel use over different appliances and technologies. For these two elements, data were taken primarily from the Eurostat fuel statistics and the IIASA GAINS model.

For the most important sources of primary PM from residential combustion, new emission factors have been established based on the available literature,

consistently taking condensable organics into account. It was found that the emission factors reported in literature are highly variable, up to a factor 10 difference was found between emission factors for the same type of installations, reflecting the high variability and dependency on measurement conditions and local circumstances. On top of the emission factors an estimate was made for so-called "bad combustion" which refers to the use of moist wood and partial load, which can have a strong impact on the emission factors. Also these numbers are again rather uncertain, but it's important to take into account such conditions as many of the small-scale wood burning may be performed by non-experienced users.

Given all the uncertainties described above, three scenarios have been defined (ideal, typical and high EF scenario) to illustrate the range of uncertainty, and to support the modelling exercise. These are the "typical" case, which is as described in the preceding paragraph, an alternative "ideal" case which excludes the impact of "bad combustion", and a "high EF" scenario in which higher emission factors are assumed than in the typical scenario. Total emissions in the typical scenario are around 40% higher than in the ideal case (in 2019), whereas resulting emissions in the "high EF" scenario are around 90% higher than in the typical scenario.

This new time-series of emissions represents the best available estimate of residential combustion emissions and changes to date, and has been used in a series of modelling studies which aim to assess the importance of these condensable organics, both for current air quality, and for trends over time. For the latter, we have restricted the modelling to the years 2010–2019 since these are the years with sufficient observational data which is suitable for trend analysis.

A number of conclusions can be drawn from the modelling:

Including condensables in a consistent way for all countries gives model results (concentrations, trends and bias) in better agreement with observations for OC and PM_{2.5} than when using the EMEP emissions which have condensables for some countries but not others.

Although the 'high' scenario seems to give the best fit to measurements in the scatter plot (Fig. 13), the agreement may reflect other factors than emissions, for example compensating for problems with dispersion modelling. Indeed, if we regard NO₂ as another semi-inert tracer of largely low-level (near ground) sources and emissions which are better constrained, there are also signs that the model underpredicts concentrations in the winter campaign period. Further, when looking at individual sites (Tables A1–A2), the NVH results are clearly too high for some sites (e.g. Norway, Italy, Spain), and other scenarios provide better results compared to the observations.

There are many factors that can contribute to such mixed results (activity data, emissions factors, assumed combustion conditions, large and small scale spatial distributions issues in emissions, dispersion and CPOA/IVOC assumptions in the modelling), and much further work (and with other observational data-sets) will be needed to disentangle the reasons for model-measurement discrepancies, and to draw conclusions on how realistic the new emissions are.

The model setup (VBS assumptions and inclusion of IVOC) also matters for $PM_{2.5}$ trends and source-receptor matrices (SRs). The underestimation of the modelled winter time (DJF) $PM_{2.5}$ trend 2010–2019 is mainly caused by underestimation of the winter time $OM_{2.5}$ trend. The higher emission (+IVOC) scenarios tend to show the largest negative trends, with better comparison to observed trends.

Assumption about volatility seems to be important for both the country-to-itself contribution, and for impacts of each country on others. In the few cases investigated so far, assuming inert CPOA provides results which generally lie within the range of the more complex VBS scenarios. Given the many uncertainties associated with the emissions and the modelling of POA and SOA, these results indicate that the inert CPOA assumptions provide a reasonable first approach for handling POA emissions, which can hopefully be improved once our understanding of the sources and processing of POA improves.

Some important caveats need to be mentioned. Firstly, 10 years of observational data is rather short for trend analysis (Aas et al., 2021), and only a few sites had the full 10 years of data; significant uncertainties remain in the calculated trend values. Secondly, the TNO Ref2_v2.1 emissions update deals only with small combustion (GNFR C) emissions, and mainly with the semivolatile compounds that affect CPOA levels. The amount of IVOC from RWC (or coal burning) that should be used is very uncertain, but its inclusion can have major impacts on modelled OC levels. Finally, other source sectors likely have IVOC that isn't in the PM or VOC inventory, so we should expect our models to underestimate OM to a certain degree. Again, the amounts involved are very uncertain.

Given these caveats, the results presented here (and indeed by any OC modelling efforts) should be considered as illustrative, rather than quantitative. There are very many issues associated with condensable organic emission estimation, as discussed in detail in Simpson et al. (2020), and equally the modelling of organic aerosol requires many unconstrained assumptions.

However, the new emission data-base, combined with increasing availability of measurements of organic and other components, should provide a good basis for future improvements in both the emission inventories and model formulations. Much analysis and further tests remain, both with the other model setups, and ideally with alternative SOA schemes to get a better idea of the sensitivity of the results to the various assumptions concerning both emissions and atmospheric processing of POA.

9. Acknowledgements

This project was funded by the Nordic Council of Ministers project (Revising historical PM_{2.5} emissions from RWC to consistently include condensable organics and assess the implications for the Gothenburg Protocol), as well as EMEP under UN-ECE. Thanks are also due to Imad El Haddad and Jianhui Jiang (PSI) and Robert Bergström (SMHI) for helping to clarify details and code of the PSI scheme, and Stephen Platt (NILU) for discussions concerning the EIMP campaign data.

A large number of people have contributed to the EMEP/COLOSSAL/ACTRIS intensive measurements period, both in the field/lab and in the data analysis. Their commitment and contribution is greatly appreciated.

10. References

- Aas, W., Fagerli, H., Yttri, K. et al., Trends in observations and EMEP MSC-W model calculations 2000–2019, in Fagerli et al. **2021**, Chap. 4, 59–106
- Amann, M., Kieseewetter, G., Schöpp, W. et al., Reducing global air pollution: the scope for further policy interventions, *Philos. Trans. Roy. Soc. A: Mathematical, Physical and Engineering Sciences*, **2020**, 378, 20190331
- Bergström, R., Denier van der Gon, H. A. C., Prévôt, A. S. H., et al., Modelling of organic aerosols over Europe (2002–2007) using a volatility basis set (VBS) framework: application of different assumptions regarding the formation of secondary organic aerosol, *Atmos. Chem. Physics*, **2012**, 12, 8499–8527
- Bruns, E. A., El Haddad, I., Slowik, J. G. et al., Identification of significant precursor gases of secondary organic aerosols from residential wood combustion, *Scientific reports, Nature Publishing Group*, **2016**, 6, 27881–27881
- Cavalli, F., Alastuey, A., Areskoug, H. et al., A European aerosol phenomenology-4: Harmonized concentrations of carbonaceous aerosol at 10 regional background sites across Europe, *Atmos. Environ.*, 2016, 144, 133–145
- Ciarelli, G., El Haddad, I., Bruns, E. et al., Constraining a hybrid volatility basis-set model for aging of wood-burning emissions using smog chamber experiments: a box-model study based on the VBS scheme of the CAMx model (v5.40), *Geosc. Mod./Dev.*, **2017a**, 10, 2303–2320
- Ciarelli, G., Aksoyoglu, S., El Haddad, I. et al, Modelling winter organic aerosol at the European scale with CAMx: evaluation and source apportionment with a VBS parameterization based on novel wood burning smog chamber experiments, *Atmos. Chem. Physics*, **2017b**, 7, 7653–7669
- Denby, B. R., Gauss, M., Wind, P., et al., Description of the uEMEPv5 downscaling approach for the EMEP MSC-W chemistry transport model, *Geosc. Mod. Dev.*, **2020**, 13, 6303–6323
- Denier van der Gon, H. A. C., Bergström, R., Fountoukis, C., et al., Particulate emissions from residential wood combustion in Europe - revised estimates and an evaluation, *Atmos. Chem. Physics*, **2015**, 15, 6503–6519
- Denier van der Gon, H., Kuenen, J. & Visschedijk, A., The TNO CAMS inventories, and alternative (Ref2) emissions for residential wood combustion, *Transboundary particulate matter, photo-oxidants, acidifying and eutrophying components. EMEP Status Report 1/2020, The Norwegian Meteorological Institute, Oslo, Norway*, **2020**, 77–82
- Donahue, N., Robinson, A., Stanier, C. & Pandis, S., Coupled Partitioning, Dilution, and Chemical Aging of Semivolatile Organics, *Environ. Sci. Technol.*, 2006, 40, 2635–2643
- Eurostat (2021), Complete energy balances (nrg_bal_c), https://appsso.eurostat.ec.europa.eu/nui/show.do?dataset=nrg_bal_c&lang=en
- Fagerli, H., Simpson, D., Wind, P. et al, Condensable organics: model evaluation and

source receptor matrices for 2018, *Transboundary particulate matter, photo-oxidants, acidifying and eutrophying components. EMEP Status Report 1/2020, The Norwegian Meteorological Institute, Oslo, Norway*, **2020**, 83–97

Fagerli, H., Tsyro, S., Simpson, D. et al., Transboundary particulate matter, photo-oxidants, acidifying and eutrophying components, *The Norwegian Meteorological Institute, Oslo, Norway*, **2021**

Gelencsér, A., May, B., Simpson, D. et al., Source apportionment of PM_{2.5} organic aerosol over Europe: primary/secondary, natural/anthropogenic, fossil/biogenic origin, *J. Geophys. Res.*, **2007**, *112*, D23S04

Grieshop, A. P., Miracolo, M. A., Donahue, N. M. & Robinson, A. L., Constraining the Volatility Distribution and Gas-Particle Partitioning of Combustion Aerosols Using Isothermal Dilution and Thermodesorption Measurements. *Environ. Sci. Technol.*, **2009**, *43*, 4750–4756

Grythe, H., Lopez-Aparicio, S., Vogt, M., et al., The MetVed model: development and evaluation of emissions from residential wood combustion at high spatio-temporal resolution in Norway. *Atmos. Chem. Phys.*, **2019**, *19*, 10217–10237

Hallquist, M., Wenger, J. C., Baltensperger, U. et al, The formation, properties and impact of secondary organic aerosol: current and emerging issues, *Atmos. Chem. Physics*, **2009**, *9*, 5155–5236

Hedberg, E., Johansson, C., Johansson, L. et al., Is levoglucosan a suitable quantitative tracer for wood burning? Comparison with receptor modeling on trace elements in Lycksele, Sweden, *J. Air Waste Manage. Assoc.*, **2006**, *56*, 1669–1678

Hodzic, A., Kasibhatla, P. S., Jo, D. S. et al., Rethinking the global secondary organic aerosol (SOA) budget: stronger production, faster removal, shorter lifetime, *Atmos. Chem. Physics*, **2016**, *16*, 7917–7941

Hoffmann, D., Tilgner, A., Iinuma, Y. & Herrmann, H., Atmospheric stability of levoglucosan: a detailed laboratory study, *Environ. Sci. Technol.*, **2010**, *44*, 694–699

IIASA, International Institute for Applied Systems Analysis, Greenhouse Gas and Air Pollution Interaction System, <https://gains.iiasa.ac.at/models/index.html>, **2021**.

Jathar, S. H., Woody, M., Pye, H. O. T. et al., Chemical transport model simulations of organic aerosol in southern California: model evaluation and gasoline and diesel source contributions, *Atmos. Chem. Phys.*, **2017**, *17*, 4305–4318

Jiang, J., Aksoyoglu, S., El-Haddad, I. et al, Sources of organic aerosols in Europe: a modeling study using CAMx with modified volatility basis set scheme, *Atmos. Chem. Physics*, **2019**, *19*, 15247–15270

Jonson, J. E., Borken-Kleefeld, J., Simpson, D. et al., Impact of excess NO_x emissions from diesel cars on air quality, public health and eutrophication in Europe, *Environ. Res. Lett.*, **2017**, *12*, 094017

Kaskaoutis, D., Grivas, G., Oikonomou, K. et al., Impacts of severe residential wood burning on atmospheric processing, water-soluble organic aerosol and light absorption, in an inland city of Southeastern Europe, *Atmos. Environ.*, **2022**, *280*, 119139

Klimont, Z., Kupiainen, K., Heyes, C. et al., Global anthropogenic emissions of

particulate matter including black carbon. *Atmos. Chem. Phys.*, **2017**, 17 (14), 8681–8723, 10.5194/acp-17-8681-2017.

Koo, B., Knipping, E. & Yarwood, G., 1.5-Dimensional volatility basis set approach for modeling organic aerosol in CAMx and CMAQ, *Atmos. Environ.*, **2014**, 95, 158–164

Kuenen, J., Dellaert, S., Visschedijk, A. et al., CAMS-REG-v4: a state-of-the-art high-resolution European emission inventory for air quality modelling, *Earth Syst. Sci. Data*, 14, 491–515, <https://doi.org/10.5194/essd-14-491-2022>, **2022**.

Matthews, B., Mareckova, K., Schindlbacher, S. et al., Emissions for 2019, in Fagerli et al. **2021**, Chap. 3, 35–55

McFiggans, G., Mentel, T. F., Wildt, J. et al., Secondary organic aerosol reduced by mixture of atmospheric vapours, *Nature*, **2019**, 565, 587–593

Mills, G., Sharps, K., Simpson, D., et al., Ozone pollution will compromise efforts to increase global wheat production, *Global Change Biol.*, **2018**, 24, 3560–3574

Murphy, B. N., Woody, M. C., Jimenez, J. L. et al., Semivolatile POA and parameterized total combustion SOA in CMAQv5.2: impacts on source strength and partitioning, *Atmos. Chem. Phys.*, **2017**, 17, 11107–11133

Murphy, B. N., Donahue, N. M., Robinson, A. L. & Pandis, S. N., A naming convention for atmospheric organic aerosol, *Atmos. Chem. Phys.*, **2014**, 14, 5825–5839

Nussbaumer, T., Czasch, C., Klippel, N et al., Particulate Emissions from Biomass Combustion in IEA Countries, Survey on Measurements and Emission Factors, *International Energy Agency (IEA), International Energy Agency (IEA) Bioenergy Task 32, Zurich, ISBN 3-908705-18-5*, **2008a**.

Nussbaumer, T., Klippel, N. & Johansson, L., Survey on Measurements and Emission Factors on Particulate Matter from Biomass Combustion in IEA Countries, 16th European Biomass Conference and Exhibition, 2–6 June 2008, Valencia, Spain, Oral Presentation OA 9.2, <http://www.verenum.ch/Publikationen/Biomass-Conf9.2.pdf>, **2008b**

Pankow, J. F., An absorption model of the gas/aerosol partitioning involved in the formation of secondary organic aerosol, *Atmos. Environ.*, **1994**, 28, 189–193

Paunu, V.-V., Karvosenoja, N., Segersson, D., et al., Spatial distribution of residential wood combustion emissions in the Nordic countries: How well national inventories represent local emissions? *Atmospheric Environment*, **2021**, 264, 118712, <https://doi.org/10.1016/j.atmosenv.2021.118712>

Platt, S. M., Yttri, K. E., Aas, W. et al., The winter 2018 intensive measurement period. A brief update Transboundary particulate matter, photo-oxidants, acidifying and eutrophying components. EMEP Status Report 1/2019, The Norwegian Meteorological Institute, Oslo, Norway, **2019**, 89–105

Platt, S., Yttri, K. E., Afif, C. et al, Source apportionment of equivalent black carbon from the winter 2017–2018 EMEP intensive measurement campaign using PMF, **2022**, <https://doi.org/10.21336/gen.h8ds-8596>

Puxbaum, H., Caseiro, A., Sánchez-Ochoa, A. et al., Levoglucosan levels at background sites in Europe for assessing of the impact of biomass combustion on the European aerosol background, *J. Geophys. Res.*, **2007**, 112, D23S05

- Robinson, A. L., Donahue, N. M., Shrivastava, M. K et al., Rethinking Organic Aerosols: Semivolatile Emissions and Photochemical Aging, *Science*, **2007**, *315*, 1259–1262
- Robinson, Al.L., Grieshop, A. P., Donahue, N. M. & Hunt, S. W., Updating the Conceptual Model for Fine Particle Mass Emissions from Combustion Systems, *J. Air & Waste Manage. Assoc.*, **2010**, *60*, 1204–1222
- Shrivastava, M. K., Lane, T. E., Donahue, N. M. et al., Effects of gas particle partitioning and aging of primary emissions on urban and regional organic aerosol concentrations, *J. Geophys. Res.*, **2008**, *113*
- Simoneit, B. R. T., A review of biomarker compounds as source indicators and tracers for air pollution, *Environ. Sci. Pollut.*, **1999**, *6*, 159–169
- Simpson, D., Gauss, M., Mu, Q. et al., Updates to the EMEP/MSC-W model, 2020–2021, in Fagerli et al. **2021**, Chap. 5, 109–121
- Simpson, D., Yttri, K., Klimont, Z. et al., Modeling Carbonaceous Aerosol over Europe. Analysis of the CARBOSOL and EMEP EC/OC campaigns, *J. Geophys. Res.*, **2007**, *112*, D23S14
- Simpson, D., Fagerli, H., Colette, A. et al., How should condensables be included in PM emission inventories reported to EMEP/CLRTAP? Report of the expert workshop on condensable organics organised by MSC-W, Gothenburg, 17–19th March 2020, *Norwegian Meteorological Institute*, **2020**, 72pp
- Szidat, S., Ruff, M., Wacker, L. et al., Fossil and non-fossil sources of organic carbon (OC) and elemental carbon (EC) in Göteborg, Sweden, *Atmos. Chem. Physics*, **2009**, *9*, 1521–1535
- Szidat, S., Jenk T.M. and Gäggl, H. et al., Radiocarbon (¹⁴C)-deduced biogenic and anthropogenic contributions to organic carbon (OC) of urban aerosols from Zürich, Switzerland, *Atmos. Environ.*, **2004**, *38*, 4035–4044
- Turpin, B. J. & Lim, H. J., Species contributions to PM_{2.5} mass concentrations: Revisiting common assumptions for estimating organic mass, *Aerosol Sci. Technol.*, **2001**, *35*, 602–610
- UNECE: Monitoring strategy for the Cooperative Programme for Monitoring and Evaluation of the Long-range Transmission of Air Pollutants in Europe for the period 2020–2029, UNECE, Geneva, Switzerland, Decision 2019/1, ECE/EB.AIR/144/Add.1, **2019**. URL: https://unece.org/fileadmin/DAM/env/documents/2019/AIR/EB_Decisions/Decision_2019_1.pdf
- UN FAO, UN Food and Agricultural Organisation, Wood energy in the ECE Region: data, trends and outlook in Europe, the commonwealth of Independent States and North America, FAO report ECE/TIM/SP/42, ISBN 9789211171549, **2017**, <https://digitallibrary.un.org/record/3823655/files/SP-42-Interactive.pdf>
- Yttri, K., Dye, C., Braathen, O.-A. et al., Carbonaceous aerosols at urban influenced sites in Norway, *Atmos. Chem. Physics*, **2009**, *9*, 2007–2020
- Yttri, K., Simpson, D., Stenström, K. et al., Source apportionment of the carbonaceous aerosol in Norway -- Quantitative estimates based on ¹⁴C, thermal-optical and organic tracer analysis, *Atmos. Chem. Physics*, **2011**, *11*, 9375–9394
- Yttri, K. E., Schnelle-Kreis, J., Maenhaut, W et al, An intercomparison study of

analytical methods used for quantification of levoglucosan in ambient aerosol filter samples, *Atmos. Measurement Techniques*, **2015**, 8, 125–147

Yttri, K. E., Simpson, D., Bergstrom, R. et al., The EMEP Intensive Measurement Period campaign, 2008–2009: characterizing carbonaceous aerosol at nine rural sites in Europe, *Atmos. Chem. Physics*, **2019**, 19, 4211–4233

Yttri, K. E., Canonaco, F., Eckhardt, S. et al., Trends, composition, and sources of carbonaceous aerosol at the Birkenes Observatory, northern Europe, 2001–2018, *Atmos. Chem. Physics*, **2021**, 21, 7149–7170

Zotter, P., Ciobanu, V. G., Zhang, Y. L. et al., Radiocarbon analysis of elemental and organic carbon in Switzerland during winter-smog episodes from 2008 to 2012 -- Part 1: Source apportionment and spatial variability, *Atmos. Chem. Phys.*, **2014**, 14, 13551–13570

Appendix

Table A1. Comparison of measured versus observed OC observations during the winter 2017/2018 intensive measurement campaign.

Site	Size	N	Obs.	NVC	(R)	NVH	(R)	NVC32	(R)	SVC32	(R)	SIVC32	(R)
AT02-Illmitz	2.5	24	3.64	-12.3	(0.29)	71.2	(0.26)	-58.4	(0.42)	-69.5	(0.47)	-50.5	(0.45)
BE07-Vielsalm	10	25	1.81	-54.5	(0.89)	-36.2	(0.88)	-52.7	(0.88)	-62.5	(0.92)	-54.7	(0.87)
CH02-Payerne	2.5	23	1.7	-30.2	(0.55)	-1.5	(0.55)	-26.2	(0.41)	-41.8	(0.50)	-16.7	(0.61)
CH33-Magadino	2.5	23	4.62	-48.1	(0.61)	-17.6	(0.62)	-3.5	(0.73)	-34	(0.67)	-2.9	(0.57)
CY02-CyprusAOs	10	82	1.46	-68.8	(0.41)	-66.1	(0.36)	-69.9	(0.29)	-70	(0.28)	-57.9	(0.17)
CZ03-Kosetice	2.5	73	3.85	-54	(0.73)	-24.3	(0.70)	-47.7	(0.59)	-57.2	(0.65)	-39.5	(0.65)
DE44-Melpitz	10	85	3.3	-63.5	(0.83)	-47.7	(0.83)	-61.7	(0.82)	-69	(0.86)	-60	(0.83)
FI36-Pallas	2.5	28	0.35	69.8	(-0.15)	93.7	(-0.12)	102.9	(-0.20)	94.6	(-0.18)	115	(-0.11)
FI50-SMEARII	10	18	1.04	0.1	(-0.08)	53	(-0.13)	75	(0.21)	30	(0.33)	46.7	(0.40)
FR09-Revin	2.5	46	1.81	-43	(0.60)	-13.8	(0.59)	-40.6	(0.55)	-59.9	(0.70)	-49.9	(0.76)
FR20-SIRTA	2.5	83	2.39	-33.9	(0.73)	3.7	(0.72)	-45.2	(0.74)	-64.3	(0.76)	-57.6	(0.78)
HU02-K-Pusztá	2.5	45	6.81	-54.4	(0.57)	-11.2	(0.56)	-52.4	(0.51)	-65.3	(0.57)	-45.6	(0.65)
IE06-Malin-Head	2.5	42	1.76	-80.7	(0.86)	-76.5	(0.86)	-77.2	(0.88)	-78.8	(0.88)	-77.3	(0.89)
IE07-Carnsore-P.	2.5	31	1.19	-71.7	(0.54)	-65.8	(0.54)	-73	(0.53)	-75.1	(0.52)	-71.9	(0.51)
IE31-Mace-Head	2.5	19	0.51	-58.8	(0.39)	-58	(0.37)	-59	(0.45)	-59.2	(0.46)	-58.9	(0.49)
IT04-Ispra	2.5	30	9.67	-34.7	(0.46)	22.1	(0.45)	-60.7	(0.50)	-72.3	(0.44)	-52.3	(0.36)
LT15-Preila	2.5	18	3.2	-75.6	(0.75)	-64.9	(0.75)	-74.2	(0.74)	-77.2	(0.76)	-69.7	(0.78)
NO02-Birkenes-II	10	13	0.52	27.9	(0.40)	81.5	(0.35)	51.9	(0.50)	1	(0.61)	15.3	(0.71)
PL05-Diablá-Góra	2.5	86	4.11	-59.8	(0.65)	-38.7	(0.66)	-60.7	(0.69)	-65.5	(0.70)	-58.8	(0.74)
RO07-Bucharest	2.5	30	8.28	-57.8	(0.76)	-23.7	(0.76)	-63.6	(0.73)	-75.3	(0.69)	-60.6	(0.58)
SE21-Hyltemossa	10	8	1.39	-42.9	(0.88)	-17.2	(0.86)	-36.5	(0.89)	-48.6	(0.92)	-35.9	(0.93)
SI08-Iskrba	2.5	72	3.31	-60.1	(0.35)	-31.2	(0.35)	-20.5	(0.08)	-47.6	(0.12)	-14	(0.11)

Notes: size refers på PM_{2,5} or PM₁₀; N to be the number of samples; Obs. gives measured concentrations in µg/m³; the remaining columns (NVC etc.) give the bias ((mod-obs)/obs) in %, and the correlation coefficient R.

Table A2. As Table A1, but for levoglucosan.

Site	Size	N	Obs.	NVC	(R)	NVH	(R)	NVC32	(R)
AT02-Illmitz	2.5	24	0.254	25.4	-0.31	174.7	(0.30)	-51.6	(0.25)
BE07-Vielsalm	10	25	0.104	-59.1	-0.61	-25	(0.62)	-58.5	(0.56)
CH02-Payerne	2.5	23	0.165	-57.8	-0.49	-26.3	(0.49)	-54.3	(0.39)
CH33-Magadino	2.5	23	0.975	-81.6	-0.57	-65.4	(0.56)	-54	(0.74)
CY02-CyprusAOs	10	31	0.014	-81.8	-0.12	-63.5	(0.12)	-81.6	(0.07)
CZ03-Kosetice	10	44	0.188	-46.2	-0.66	8.8	(0.66)	-34.8	(0.48)
DE44-Melpitz	10	85	0.183	-67.7	-0.67	-39.3	(0.68)	-63.6	(0.71)
FI36-Pallas	2.5	28	0.012	-34.2	-0.05	30.5	(0.05)	16.5	(-0.36)
FI50-SMEARII	10	18	0.041	51.4	(-0.28)	198.4	(-0.29)	220.8	(0.10)
FR09-Revin	2.5	46	0.14	-45.7	-0.48	-1.8	(0.49)	-43.1	(0.47)
FR20-SIRTA	2.5	61	0.404	-65.5	-0.44	-38.2	(0.44)	-73.3	(0.41)
HU02-K-Pusztá	2.5	35	0.534	-54.8	-0.72	-0.9	(0.73)	-51.7	(0.69)
IE06-Malin-Head	2.5	39	0.043	-87.7	-0.84	-76.1	(0.84)	-85.8	(0.87)
IE07-Carnsore-P.	2.5	30	0.04	-85.8	-0.48	-72.6	(0.48)	-86.9	(0.48)
IE31-Mace-Head	2.5	7	0.011	-96.9	-0.24	-94	(0.24)	-97	(0.28)
IT04-Ispra	2.5	30	1.5	-56.4	-0.47	-13.6	(0.47)	-74.9	(0.45)
LT15-Preila	2.5	18	0.151	-80.4	-0.72	-61.5	(0.71)	-79	(0.69)
NO02-Birkenes-II	10	13	0.014	143	-0.22	352.8	(0.24)	260.5	(0.47)
PL05-Diablo-Gora	2.5	30	0.134	-59.8	-0.72	-22.3	(0.71)	-60.3	(0.67)
RO07-Bucharest	2.5	30	1.107	-65.8	-0.74	-33.4	(0.74)	-71.3	(0.71)
SE21-Hyltemossa	10	8	0.05	-38.8	-0.78	23.2	(0.78)	-26.2	(0.82)
SI08-Iskrba	2.5	33	0.2	-46.3	-0.26	11.5	(0.28)	52.3	(0.11)

Table A3. As Table A1, but for EC.

Site	Size	N	Obs.	NVC	(R)	NVH	(R)	NVC32	(R)
AT02-Illmitz	2.5	24	0.68	32.4	(0.39)	159,3	(0.37)	-31,7	(0.40)
BE07-Vielsalm	10	25	0.17	54.2	(0.68)	109,2	(0.66)	54,8	(0.68)
CH02-Payerne	2.5	23	0.4	2.5	(0.26)	41.3	(0.25)	11	(0.08)
CH33-Magadino	2.5	23	1.21	-39.7	(0.34)	-10.1	(0.33)	-17.7	(0.50)
CY02-CyprusAOs	10	82	0.29	-76.1	(0.39)	-72.1	(0.34)	-78	(0.24)
CZ03-Kosetice	2.5	73	0.9	-43.4	(0.53)	-7.6	(0.48)	-36	(0.38)
DE44-Melpitz	10	85	0.52	-19.3	(0.70)	10.1	(0.72)	-3.5	(0.72)
FI36-Pallas	2.5	28	0.05	-41.2	(0.27)	-7.4	(0.23)	-21.2	(0.10)
FI50-SMEARII	10	18	0.13	96.4	(-0.23)	190.1	(-0.26)	287.1	(0.02)
FR09-Revin	2.5	46	0.22	43.7	(0.40)	106.5	(0.39)	48.7	(0.39)
FR20-SIRTA	2.5	83	0.5	6.1	(0.80)	50.5	(0.78)	-11.7	(0.80)
HU02-K-Pusztza	2.5	45	1.45	-48.3	(0.51)	2.2	(0.50)	-46.5	(0.44)
IE06-Malin-Head	2.5	42	0.25	-77.8	(0.77)	-69.5	(0.78)	-68.5	(0.82)
IE07-Carnsore-P.	2.5	31	0.24	-77.6	(0.44)	-70.3	(0.44)	-79.6	(0.43)
IE31-Mace-Head	2.5	19	0.03	-79.6	(0.38)	-74.9	(0.37)	-81.1	(0.39)
IT04-Ispra	2.5	30	1.73	-11.8	(0.49)	58.6	(0.48)	-49.8	(0.44)
LT15-Preila	2.5	18	0.3	-28.2	(0.61)	5.8	(0.61)	-20.4	(0.58)
NO02-Birkenes-II	10	13	0.06	78.1	(0.62)	162.1	(0.57)	158.3	(0.69)
PL05-Diablo-Gora	2.5	86	0.55	10.8	(0.67)	67	(0.68)	7.3	(0.70)
RO07-Bucharest	2.5	30	1.01	-33.7	(0.69)	17.1	(0.67)	-42.7	(0.47)
SE21-Hyltemossa	10	8	0.18	6.3	(0.75)	55.1	(0.77)	29.1	(0.75)
SI08-Iskrba	2.5	72	0.26	25.2	(0.24)	120.4	(0.26)	170.5	(0.11)

About this publication

Revising PM_{2.5} emissions from residential combustion, 2005–2019

Implications for air quality concentrations and trends

David Simpson, Jeroen Kuenen, Hilde Fagerli, Daniel Heinesen, Anna Benedictow, Hugo Denier van der Gon, Antoon Visschedijk, Zbigniew Klimont, Wenche Aas, Yong Lin, Karl Espen Yttri, Ville-Veikko Paunu

ISBN 978-92-893-7357-9 (PDF)

ISBN 978-92-893-7358-6 (ONLINE)

<http://dx.doi.org/10.6027/temanord2022-540>

TemaNord 2022:540

ISSN 0908-6692

© Nordic Council of Ministers 2022

Cover photo: Ricardo Prospero / Unsplash

Published: 31/8/2022

Disclaimer

This publication was funded by the Nordic Council of Ministers. However, the content does not necessarily reflect the Nordic Council of Ministers' views, opinions, attitudes or recommendations.

Rights and permissions

This work is made available under the Creative Commons Attribution 4.0 International license (CC BY 4.0) <https://creativecommons.org/licenses/by/4.0>.

Translations: If you translate this work, please include the following disclaimer: This translation was not produced by the Nordic Council of Ministers and should not be construed as official. The Nordic Council of Ministers cannot be held responsible for the translation or any errors in it.

Adaptations: If you adapt this work, please include the following disclaimer along with the attribution: This is an adaptation of an original work by the Nordic Council of Ministers. Responsibility for the views and opinions expressed in the adaptation rests solely with its author(s). The views and opinions in this adaptation have not been approved by the Nordic Council of Ministers.

Third-party content: The Nordic Council of Ministers does not necessarily own every single part of this work. The Nordic Council of Ministers cannot, therefore, guarantee that the reuse of third-party content does not infringe the copyright of the third party. If you wish to reuse any third-party content, you bear the risks associated

with any such rights violations. You are responsible for determining whether there is a need to obtain permission for the use of third-party content, and if so, for obtaining the relevant permission from the copyright holder. Examples of third-party content may include, but are not limited to, tables, figures or images.

Photo rights (further permission required for reuse):

Any queries regarding rights and licences should be addressed to:
Nordic Council of Ministers/Publication Unit
Ved Stranden 18
DK-1061 Copenhagen
Denmark
pub@norden.org

Nordic co-operation

Nordic co-operation is one of the world's most extensive forms of regional collaboration, involving Denmark, Finland, Iceland, Norway, Sweden, and the Faroe Islands, Greenland and Åland.

Nordic co-operation has firm traditions in politics, economics and culture and plays an important role in European and international forums. The Nordic community strives for a strong Nordic Region in a strong Europe.

Nordic co-operation promotes regional interests and values in a global world. The values shared by the Nordic countries help make the region one of the most innovative and competitive in the world.

The Nordic Council of Ministers
Nordens Hus
Ved Stranden 18
DK-1061 Copenhagen
pub@norden.org

Read more Nordic publications on www.norden.org/publications